An accurate analytic H_4 potential energy surface

A. I. Boothroyd, P. G. Martin, and W. J. Keogh*
Canadian Institute for Theoretical Astrophysics, University of Toronto, Toronto, Ontario, M5S 3H8, Canada

M. J. Peterson†
Department of Chemistry, University of Toronto, Toronto, Ontario, M5S 3H6, Canada
(October 5, 2001: J. Chem. Phys., in press)

Abstract

The interaction potential energy surface (PES) of H_4 is of great importance for quantum chemistry, as a test case for molecule-molecule interactions. It is also required for a detailed understanding of certain astrophysical processes, namely collisional excitation and dissociation of H_2 in molecular clouds, at densities too low to be accessible experimentally. The 6101 *ab initio* H_4 energies reported in 1991 by Boothroyd *et al.* demonstrated large inaccuracies in analytic H_4 surfaces available at that time. Some undesirable features remained in the more accurate H_4 surfaces fitted to these energies by Keogh and by Aguado *et al.*, due in part to the relatively sparse coverage of the 6-dimensional H_4 conformation space afforded by the 6101 *ab initio* energies. To improve the coverage, 42079 new *ab initio* H_4 energies were calculated, using Buenker's multiple reference (single and) double excitation configuration interaction (MRD-CI) program. Here the lowest excited states were computed as well as the ground state, and energies for the original 6101 conformations were recomputed. The *ab initio* energies have an estimated rms "random" error of ~ 0.5 millihartree and a systematic error of ~ 1 millihartree (0.6 kcal/mol).

A new analytical H_4 PES was fitted to these 48180 *ab initio* energies (and to an additional 13367 points generated at large separations), yielding a significant improvement over previous H_4 surfaces. This new PES has an rms error of 1.43 millihartree relative to these 48180 *ab initio* energies (the fitting

*Present address: i-STAT Canada Ltd., 436 Hazeldean Road, Kanata, Ontario, K2L 1T9, Canada.

†Present address: Department of Computing and Networking Services, University of Toronto, Toronto, Ontario, M5S 3J1, Canada.

procedure used a reduced weight for high energies, yielding a weighted rms error of 1.15 millihartree for these 48180 *ab initio* energies). For the 39064 *ab initio* energies that lie below twice the H_2 dissociation energy, the new PES has an rms error of 0.95 millihartree. These rms errors are comparable to the estimated error in the *ab initio* energies themselves. The new PES also fits the van der Waals well to an accuracy of about 5%. For relatively compact conformations (energies higher than the H_2 dissociation energy), the conical intersection between the ground state and the first excited state is the largest source of error in the analytic surface. The position of this conical intersection forms a somewhat complicated 3-dimensional hypersurface in the 6-dimensional conformation space of H_4. A large portion of the position of the conical intersection has been mapped out, but trying to include the conical intersection explicitly in an analytic surface is beyond the scope of the present paper.

I. INTRODUCTION

The interaction potential energy surface (PES) of H_4 (i.e., four hydrogen atoms) is of great importance for quantum chemistry. Available *ab initio* potential energy surfaces for H_3 and for $H_2 - He$ serve as important test cases of theories of the interaction of a molecule with a single atom. H_4 is the simplest, and yet a crucial, test case for a basic understanding of intermolecular energy transfer and chemical reactions between molecules, and for checking rigorous theoretical predictions against experimental results. It is highly desirable to have a PES for H_4 that attains or at least approaches the "chemical accuracy" (of order one millihartree, i.e., better than one kcal/mole) required for reaction dynamics. The *ab initio* energy computations of Boothroyd *et al.*[1] enabled analytic H_4 surfaces to approach this goal[2–5]; this paper reports a greatly-expanded set of *ab initio* energies, and an improved H_4 PES fitted to these energies.

The H_4 PES is also of particular astrophysical interest for studying $H_2 - H_2$ interactions in physical conditions not accessible to experiment, namely the low densities characteristic of giant molecular clouds in the interstellar medium, where star formation occurs. Heating of these clouds by strong shock waves causes rotational and vibrational excitation of the H_2 molecules, and can lead to collision-induced dissociation of H_2 into free H atoms. The collision rates in molecular clouds can be so low that the (observed) forbidden (quadrupole) infrared emission of excited H_2 molecules can induce highly non-thermal distributions over the internal states of H_2 (see, e.g., Refs. 6, 7, and 8). Because the mean free paths of molecules are thousands of kilometers at such low densities, these processes will remain inaccessible to laboratory experiment. Computer simulation is therefore a *sine qua non* in the study of the physics and chemistry of star forming regions.

The van der Waals well of $H_2 + H_2$ has been extensively studied, and very accurate PES's are available for this restricted region of H_4. The rigid-rotor $H_2 + H_2$ PES of Schaefer and Köhler[9] is almost identical to that reported a decade later by Diep and Johnson[10], but these $H_2 + H_2$ PES's are valid only for H_2 molecules of near-equilibrium size with relatively large intermolecular separations $R \gtrsim 2$ Å (corresponding to interaction energies

$\lesssim$ 10 kcal/mol). Billing and Kolesnick[11] combined an older 7-parameter long-range $H_2 + H_2$ interaction potential[12] with a 6-parameter $H_2 + H_2$ fit to the 85 *ab initio* H_4 energies of Schwenke[13] (which lay mostly in the region of the $H_2 + H_2$ repulsive wall), but fitted these latter points two or three times worse than Schwenke's own surface did[11,13].

Boothroyd *et al.*[1] reported 6101 *ab initio* H_4 energies, providing for the first time full (albeit relatively sparse) coverage of the entire 6-dimensional conformation space of H_4 that can be reached by a pair of H_2 molecules colliding with sufficient energy to dissociate one or both of the molecules. They demonstrated that even the best H_4 PES available at that time (that of Schwenke[13]) had errors more than an order of magnitude worse than the wished-for "chemical accuracy" in the $H_2 + H_2$ interaction region. However, the 6101 *ab initio* H_4 energies provided sufficient information to fit an H_4 PES that could approach "chemical accuracy", and this was done both by Keogh[2] (using an extension of Schwenke's[13] approach to fitting H_4) and by Aguado *et al.*[3] (using a many-body expansion); a slightly-improved version of Keogh's PES was developed and used by Martin *et al.*[4] and Mandy *et al.*[5] for quasi-classical trajectory calculations of $H_2 + H_2$ interactions. Some undesirable features remained in these more-accurate H_4 surfaces, due in part to the relatively sparse coverage of the 6-dimensional H_4 conformation space afforded by the 6101 *ab initio* energies.

In the present work, we have computed 42079 new *ab initio* H_4 energies to improve the coverage of the H_4 conformation space. We have also recomputed the original 6101 *ab initio* energies (nine erroneous energy values were found and corrected). Both the ground state energy and the first few excited state energies were computed, and a large portion of the conical intersection of the ground state with the first excited state was mapped out. A new H_4 PES was fitted to the 48180 ground-state *ab initio* energies (and to an additional 13367 points generated to constrain the fit at very large and at very small separations), yielding a significant improvement over the previous H_4 surfaces.

II. METHODS

Atomic units are used in this paper unless otherwise specified, i.e., distances are in bohrs (a_0) and energies are in hartrees (E_h), millihartrees (mE_h), or microhartrees (μE_h). Recall that 1 a_0 = 0.529177 Å, while 1 mE_h = 0.0272114 eV = 0.62751 kcal/mole.

Unless otherwise stated, energy values are measured relative to the energy of four isolated hydrogen atoms; thus an energy $E = 0.0\ E_h$ lies about twice the H_2 dissociation energy above the energy of two isolated equilibrium H_2 molecules.

A. The grid of conformations to be fitted

The relative positions of the four hydrogen atoms in any specific conformation can be expressed in terms of six independent relative coordinates. We defined our main grids in conformation space in terms of three distances (A, B, and C) and three angles (θ, ψ, and ϕ); for convenience in referring to them we numbered the hydrogen atoms as atom-1 through atom-4, and also defined a set of Cartesian coordinates, atom-i lying at (x_i, y_i, z_i) (see Boothroyd *et al.*[1]). By definition, $A \equiv r_{12}$ is the shortest of the 6 interatomic distances, and lies along the z-axis centered on the origin; $B \equiv r_{23}$ is the shortest of the remaining

5 distances, except possibly for $C \equiv r_{34}$. Atom-3 lies in the upper-right quadrant of the y-z plane, at an angle θ about the origin relative to the z-axis ($0 \leq \theta \leq \pi/2$). The projection of C on the y-z plane makes an angle ϕ about atom-3 relative to the positive z-direction ($-\pi < \phi \leq \pi$), and C itself lies at an angle ψ relative to the y-z plane ($0 \leq \psi \leq \pi/2$). Note that different distance and angle definitions were used in the analytic surface (see § II C).

The original 6101 conformations of H_4 described in Boothroyd *et al.*[1] were used (these included 87 conformations with energies computed by Schwenke[13,14]). Improved *ab initio* energies were computed for all of these original conformations (note that 9 of the energies reported by Boothroyd *et al.*[1] were in error by 2 mE_h or more: see § II B). These original 6101 conformations were supplemented by *ab initio* energies computed at 42079 new conformations, to improve coverage of conformation space and to constrain the analytic surface in regions where the original fit of Keogh[2] tended to have unphysical features (this yielded a total of 48180 conformations with *ab initio* H_4 energies). An additional 13367 conformations were generated to constrain the fit in regions where the energy could not be obtained directly from an *ab initio* H_4 computation (see § II A 6, II A 7, and II A 8), for a total of 61547 fitted conformations.

1. The main grid

The original main grid of Boothroyd *et al.*[1] had contained 5832 conformations (which had been supplemented by 182 "test" conformations and the 87 Schwenke[13,14] conformations to yield the original total of 6101 conformations). This original main grid was enlarged by adding three new distance values (0.8, 4.0, and 5.0 a_0); the enlarged grid thus contains the original grid of 5832 conformations as a subset, along with 7968 new conformations. In this enlarged grid, the three distances described above (A, B, and C) were thus chosen from among the enlarged set of ten values {0.6, 0.8, 1.0, 1.4, 1.75, 2.1, 2.6, 3.4, 4.0, 5.0 a_0}, although only one of the three distances was allowed to be as small as 0.6 a_0. (If the direction of the third distance C was back towards the first two atoms, the distance C was lengthened as necessary to put the fourth atom on the far side of the first two atoms.) As before, the three angles described above (θ, ψ, and ϕ) were chosen at 30 degree intervals, unless one of the three distances was short (0.6 a_0) or long ($\geq$ 3.4 a_0), in which case angles were at 45 degree intervals. For an "out-of-plane" angle $\psi = 60$ degrees, the corresponding azimuthal angle ϕ was stepped by 90 degrees, to avoid excessively closely-spaced points (note that for $\psi = 90$ degrees the angle ϕ is irrelevant). Care was taken to eliminate duplicate (and almost-duplicate) conformations.

For the new conformations (those containing distances of 0.8, 4.0, or 5.0 a_0), the actual grid position was "fuzzed out" in distances and angles. For the three distances (A, B, and C), the permitted range reached half-way to the next-lower and next-higher distance values; for the three angles (θ, ψ, and ϕ), the permitted range was centered on the angular grid value with a size equal to the angular grid spacing (30 or 45 degrees, depending on the distances, as described above). Random values of the six coordinates were chosen uniformly in these permitted ranges, i.e., the "fuzzed" grid-point lay randomly in the six-dimensional "box" in conformation space defined by "those conformations lying closer to the grid point than to any neighboring grid point." Certain coordinates were in some cases excepted from

this "fuzzing," such that planar conformations were not made non-planar, equilateral- and isosceles-triangle sub-conformations of the first three atoms were not made scalene, and linear conformations were not made non-linear. The "fuzzing" was intended to reduce the room for oscillations in the analytic surface between grid points. (Note that this "fuzzing" was *not* done for the original grid of Boothroyd *et al.*[1]).

An additional 190 conformations of high symmetry were computed, with distances as in the above enlarged grid; these comprised squares (D_{4h}), rectangles (D_{2h}), "pyramids" on an equilateral triangle base (C_{3v}, or higher symmetry for tetrahedra and "flattened pyramids" of height zero), and "T-shapes" (C_{2v}: linear symmetric H_3 with a fourth H atom at right angles from the center). These supplemented the high-symmetry cases that comprised many of the 182 old "test" conformations of Boothroyd *et al.*[1] (note that the 87 conformations where Schwenke's energies were used[1,13,14] were also of symmetry C_{2v} or higher).

The above grid was initially supplemented by 1940 "random" H_4 conformations, where distances A, B, C (between 0.7 and 5.0 a_0) and angles θ, ψ, ϕ were obtained randomly (but not completely uniformly, in order to provide a coverage of conformation space not too different from that of the above grid: i.e., intermediate and short distances were favored over long ones, there was a significant probability of two distances being equal, and there was a significant probability of obtaining a planar conformation). These conformations were intended to provide coverage between grid points of the original grid.

2. Conformations tending towards $H_3 + H$

A grid of 2320 conformations tending towards H_3+H was computed, since the interaction energy between H_3 and H is non-negligible out to longer separations than is the case for $H_2 + H_2$ or $H_2 + H$. The shortest distance (A) was chosen from {0.6, 0.8, 1.0, 1.4, 1.75, 2.1, 2.6 a_0}, and the next-shortest (B) from {0.8, 1.0, 1.4, 1.75, 2.1, 2.6, 3.4, 4.0, 5.0 a_0} (to comprise the "H_3"); the long distance (C, roughly the distance from the fourth H atom to the nearest atom in the "H_3") was chosen from {6.0, 7.0, 8.4 a_0}. Angles were at 45 degree intervals; these grid points were also "fuzzed" as described above. Conformations in regions already sampled by the main H_4 grid were omitted.

This grid was supplemented by 174 higher-symmetry cases, comprising either an equilateral-triangle or linear-symmetric H_3 (with distances {0.8, 1.0, 1.4, 1.75, 2.6 a_0}) and a fourth H atom at a fairly large distance from the center (distances {5.0, 6.0, 7.0, 8.0, 9.0, 10.0, 11.0 a_0} in most cases; the largest pyramid height was actually 9.999999 a_0). The triangles thus yielded "pyramids" as well as "Y-shaped" and "kite-shaped" planar C_{2v} conformations, while the linear H_3 yielded linear and "T-shaped" conformations.

3. Fairly compact conformations

To constrain the fitted surface in regions where it tended to have unphysical features[2], a set of 1262 fairly compact conformations of high symmetry was computed. These were made up of a small H_2 (of sizes {0.6, 0.8, 1.0, 1.4 a_0}) and a large H_2 (of sizes {1.75, 2.1, 2.6, 3.0, 3.4, 4.0, 5.0, 6.0, 7.0 a_0}) with a small separation between their centers ({0.0, 0.5, 1.0, 1.5, 2.0, 2.75 a_0}). The two H_2's were either parallel (yielding trapezoids) or "crossed"

(forming a diamond shape for zero $H_2 - H_2$ separation); in the latter case, the displacement was either along the axis of the shorter H_2 (yielding "Y-shapes") or perpendicular to both H_2 axes (yielding a non-planar "crossed" conformation). Excessively compact conformations were omitted, i.e., conformations with any distance below 0.5 a_0, or with a small H_2 of 0.6 a_0 and another distance below 0.7 a_0. In addition, 640 variants were also computed, by taking one of the above conformations at random and shifting the larger H_2 along its own axis by a relatively small amount. None of these conformations were "fuzzed".

4. Large set of "random" conformations

After a number of preliminary fits had been made, 27585 additional "random" H_4 conformations were computed. Distances A, B, C (between 0.7 and 5.0 a_0) and angles θ, ψ, ϕ were obtained randomly (but non-uniformly); unlike the "random" conformations of § II A 1, the probability distributions for these additional conformations were chosen to emphasize the region of conformation space that was expected to be sampled by typical $H_2 + H_2$ dissociative collisions (H_4 energies below twice the H_2 dissociation energy, i.e., below the energy of four isolated H-atoms). Also, for conformations tending towards $H_3 + H$ (namely, with $C > 1.5 \max\{A, B\}$), the range for C was extended such that the maximum allowed distance for C became 8.0 a_0 rather than 5.0 a_0 (to sample the cases tending towards $H_3 + H$ with non-negligible interaction energy between the H_3 and the H).

Only about 6% of this set of 27585 "random" conformations were planar, and only about 0.3% of the planar conformations were linear. Compare this to the earlier 20595 conformations (described in § II A 1 through II A 3), where the relatively coarse angular grid meant that 48% of the conformations were planar, and 9% of the planar conformations were linear (note that very nearly the same proportions hold true for the main grid of § II A 1 alone, and for the original points of Boothroyd *et al.*[1]).

5. Mapping of conical intersection with excited state

As discussed in more detail below in § III A, a considerable effort was made to map out any conical intersections where the ground state and the first excited state meet. Since the intersection proved much more complex than we had at first realized, a total of 13356 *ab initio* energies were computed during the mapping process. These were *not* included in the fit, since they were concentrated in only a small sub-volume of the total conformation space and would have distorted the fit by vastly over-emphasizing that sub-volume at the expense of the rest of the conformation space.

6. Non–ab-initio $H_2 + H_2$ conformations for the van der Waals well

For $H_2 + H_2$ with intermolecular separations greater than about 5 a_0, the estimated uncertainty became far from negligible compared to the interaction energy; also, this region of the H_4 PES has been studied by many other investigators. In particular, the rigid-rotor $H_2 + H_2$ PES of Schaefer and Köhler[9], based on both *ab initio* computations and

experimental results, should certainly be quite accurate in this region; for example, it may be seen to be in good agreement with the accurate *ab initio* computations (over a range of intermolecular separations) of Burton and Senff[15,16] and of Senff and Burton[17], as well as with the experimental results of Buck *et al.*[18–20]. Our H_4 surface does not fit the $H_2 + H_2$ van der Waals well sufficiently accurately to justify updating to a more recent rigid-rotor $H_2 + H_2$ PES, such as that of Diep and Johnson[10] (which differs from the Schaefer and Köhler[9] surface by only a few μE_h in the region of the van der Waals well). We thus used the Schaefer and Köhler[9] formula to obtain energies of 3611 conformations in the $H_2 + H_2$ van der Waals well, which were given a relatively high weight in the fit to reflect their high accuracy and the small depth of the van der Waals well (see § II D 1); these were referred to as "S&K-H_2+H_2" conformations, and were generated as described below.

For H_2 molecules of size $r_a = r_b = 1.449\ a_0$, the separation R between their centers was chosen from {4.5, 5.0, 5.5, 6.0, 6.5, 7.0, 7.5, 8.0, 9.0, 10.0, 11.0, 13.0, 16.0, 20.0 a_0}, and relative orientations of the H_2 molecules were generally considered at 45 degree intervals (for some separations, 22.5 degree intervals were used) — orientations were defined in terms of Schaefer and Köhler's modified Jacobi angles θ_1, θ_2, and ϕ, where $\cos\theta_1 = \vec{r}_a \cdot \vec{R}/(r_a R)$, $\cos\theta_2 = -\vec{r}_b \cdot \vec{R}/(r_b R)$, and $\cos\phi = (\vec{r}_a \times \vec{R}) \cdot (\vec{r}_b \times \vec{R})/(|\vec{r}_a \times \vec{R}||\vec{r}_b \times \vec{R}|)$. The Schaefer and Köhler[9] formula was not designed for non-equilibrium H_2 molecule sizes, but these were still needed to constrain our analytic H_4 surface. We thus considered H_2 molecules of sizes chosen from {0.6, 0.8, 1.0, 1.2, 1.449, 1.75, 2.1, 2.6, 3.4 a_0}, but with fewer intermolecular distances and fewer orientations for sizes other than 1.449 a_0 (and lower weight in the fit: see § II D 1). Our *ab initio* energies indicated that the position of the van der Waals well and its repulsive wall varied with the size of the H_2 molecules; to approximate this effect, the Schaefer and Köhler[9] formula was modified slightly, such that its repulsive wall joined smoothly onto that from the *ab initio* energies.

The original Schaefer and Köhler[9] surface is written in terms of functions of the intermolecular separation R multiplied by functions of the orientation angles. This formula was modified in two ways. (i) The intermolecular distance R used in their formula was increased for small H_2 molecule sizes, and decreased for large H_2 sizes where the H_2 molecules were inclined towards each other (i.e., if the shortest distance B between atoms in different molecules was less than would be the case for equilibrium H_2 sizes); this improved the agreement with the position of the repulsive wall. Note that conformations were discarded altogether if the shortest distance B between atoms in different molecules was too small, namely, $B < 3.5\ a_0$ for $r_a = r_b = 1.449\ a_0$, $B < 4\ a_0$ for $1.2\ a_0 \leq \{r_a, r_b\} \leq 1.75\ a_0$, $B < 5\ a_0$ for $\max\{r_a, r_b\} = 3.4\ a_0$, and $B < 4.5\ a_0$ otherwise. (ii) For small H_2 molecule sizes, the anisotropic terms were reduced, since a small H_2 molecule should look more nearly spherical. Note that Diep and Johnson[10] computed rigid-rotor $H_2 + H_2$ potentials for H_2 molecule sizes of both 1.449 a_0 and 1.402 a_0; their figures 11 and 12 suggest that the latter case is slightly less anisotropic, in qualitative agreement with modification (ii). A detailed description of the modified Schaefer/Köhler formula is presented in Appendix A in EPAPS[21].

Note that this modified version of the Schaefer/Köhler formula does not have continuous derivatives and is thus not suited for use as an actual H_4 surface. However, it is adequate for generating constraining conformations at discrete distances, to give a general guide as to the position of the van der Waals well for our H_4 fit.

7. Non–ab-initio very compact conformations

To ensure that *extrapolation* of our fitted H_4 surface to very short distances is reasonably well behaved, we added a grid of 1197 *extremely* compact conformations with distances chosen from $\{0.4, 0.6, 1.0, 1.4, 1.75, 3.4\ a_0\}$; either just one distance was as short as 0.4 a_0, or at least two distances were 0.6 a_0. Angles were incremented by 30 degrees, unless at least one distance was 0.4 or 3.4 a_0, in which case they were incremented by 45 degrees. As we did in constraining the BKMP2 H_3 PES[22], energies were estimated via the (non-Johnson-corrected, non-cusp-rounded) London formula (see § II C 1) and were given very low weight in the fit (see § II D 1; the lowest energy of this set of points was 0.464 E_h and the highest was 2.690 E_h. Although the energies calculated via the London equation are quite inaccurate compared to *ab initio* energies, these points (with an appropriately reduced weight) can guide the surface in this region of very compact geometries and prevent it from turning back over and decreasing in energy. These were referred to as "H_4London" conformations.

8. Semi– and non–ab-initio $H_3 + H$ conformations

Finally, the H_4 PES must reduce asymptotically to the H_3 PES as the fourth atom is moved off to a large distance from the first three atoms. As a basis we took the 8559 H_3 conformations of BKMP2[22]: the 542 of the preliminary grid, the 6548 of the comprehensive grid (2 being duplicates of preliminary grid points), and the 503 of Partridge *et al.*[23,24] — all 7951 of these have *ab initio* energies (of higher accuracy than the H_4 *ab initio* energies) — as well as the 968 H_3 van der Waals conformations generated from the MTT formula[22] fitted to Partridge's energies. We then added a fourth H atom at a random position, from 9 to 16 a_0 from the nearest atom in H_3, or slightly further for reasonably compact H_3 distances r_i: this allowed range was shifted outwards by $0.6 \max\{0.0\ a_0\ ,\ 8\ a_0 - (r_1 + r_2 + r_3)\}$ (e.g., for $r_1 = r_2 = r_3 = 1.5\ a_0$, the fourth atom would lie in the range from 11.1 to 18.1 a_0). Our *ab initio* energies for conformations tending towards $H_3 + H$ suggested that, even at the lower end of this range of distances, interaction energies for the fourth atom relative to the first three would be less than the "random" error of $\sim 0.1\ mE_h$ in the H_3 *ab initio* energies, and much less than the systematic H_3 error of $\sim 0.4\ mE_h$ estimated in BKMP2[22]. Thus for these 8559 $H_3 + H$ conformations we simply adopted the H_3 energy; they are referred to as "H_4fromH_3" conformations. They were given increased weights in the fit to reflect the higher accuracy both of their energies and of the BKMP2 H_3 surface which the H_4 surface asymptotically approaches.

B. Ab initio computations and analysis

1. Computational methods and CPU-time

The *ab initio* computations and analysis of errors largely follow the methods described in our previous papers[1,22,25]. Earlier H_4 energies[1] had been computed using a Cray version of Buenker's MRD-CI program[26]; subsequent energies were computed using a workstation version[27]. The $(9s3p1d)/[4s3p1d]$ Gaussian basis set from Siegbahn and Liu[28] was used,

as in Boothroyd *et al.*[1] (see Appendix B in EPAPS[21] for more details). For most conformations, molecular orbitals were obtained from closed shell SCF, as before[1]; if closed shell SCF iterations were slow to converge, open shell SCF or mixed (1 closed, 2 open) shell SCF was automatically used instead (for several hundred conformations, energies were computed using molecular orbitals from two or three different SCF types). A configuration selection threshold of $T = 10\ \mu E_h$ was used for most points (Buenker's MRD-CI program automatically extrapolates to zero threshold, using truncated-CI energies at T and at $2T$ plus a parameterization of the estimated effects of neglected configurations). Multiple CI roots were computed, to ensure that the ground state energy was always among the energies reported by the program. A fairly extensive set of reference configurations was used for the CI calculation: the minimum size of C_R^2 (the sum of reference configuration C^2 values) was 0.927, and the *average* size was 0.974. (Note that additional reference configurations were included automatically if the program estimated that they would increase C_R^2 by more than 0.001 individually and by more than 0.003 collectively).

The above relatively small basis set and relatively large selection threshold were required by CPU-time considerations (and also yielded energies consistent with our previous H_4 *ab initio* computations[1]). So long as the *ab initio* energies are of accuracy comparable to the desired "chemical accuracy," the most important factor in obtaining a good fitted analytic surface is adequate coverage in the 6-dimensional conformation space of H_4, which requires large numbers of *ab initio* energies. In the late 1980's, only a generous grant of time on a Cray X/MP enabled computation of the original 6101 *ab initio* energies of Boothroyd *et al.*[1], even though only a single CI root was computed for each. By the time when the points of the current work were computed (in the late 1990's), the workstation version of Buenker's MRD-CI program proved to have comparable speed. Nonetheless, a total of over 5 years of CPU-time plus I/O-time was required for the 74134 *ab initio* energies that were computed in the present work (this includes all recomputations, as well as the points used to look for the conical intersection). These computations were distributed among about a dozen different computers, mostly workstations of various types, but including a couple of high-performance machines. For the faster computers the I/O-time tended to dominate (due to large temporary files), but there was one exception to this: more than half of the energies were computed on a single high-end SGI with a fast disk, which allowed computation of a typical *ab initio* energy in about 10 minutes. The other computers typically required 30 to 60 minutes per point, with some older machines requiring up to several hours per point.

2. Errors in nine earlier points

Aguado *et al.*[3,29] pointed out that a few of the earlier energies of Boothroyd *et al.*[1] were in error for high-symmetry conformations, lying at the first excited state energy rather than the ground state energy. We thus recomputed the energies of those points where only one MRD-CI root had been computed, having the MRD-CI program compute the lowest 5 roots, to check for such errors. We first recomputed all high-symmetry conformations (D_{4h}, D_{3h}, D_{2h}, $D_{\infty h}$, D_{2d}, C_{3v}, C_{2v}, $C_{\infty v}$, C_{2h}), all points where the SCF iterations had been slow to converge or where closed shell SCF had not been used, all points that had a difference of more than 1.5 mE_h between two computed energies (with different SCF-types or different

reference sets), and all points differing by more than 4 mE_h from the then-current fitted analytic H_4 surface of Keogh[2] (which had an rms of about half that); these cases comprised 1149 of our 6101 previously-computed points. Of these 1149 points, only 9 were found to have been in error by more than $\sim$ 2 mE_h, with 7 having yielded the first excited state ($\sim$ 24.2, 23.6, 21.2, 14.8, 4.8, 3.9, and 2.5 mE_h above the respective ground states), and 2 with errors of 3.8 and 3.4 mE_h still lying much nearer the ground state than the first excited state. It seemed worthwhile to test *all* the remaining single-root energies, by recomputing with multiple roots the remaining 4952 points from the original grid, as well as the 12000 points from the new grid (that had at that time already been computed with the workstation MRD-CI program). Of these 16952 points, *none* were found to have had erroneous single-root energies. The 2494 conformations of "H_4 tending towards $H_3 + H$" were all computed with multiple roots in the first place, as were the 20595 conformations of the "random" H_4 grid.

3. Small corrections applied to the MRD-CI energies

Using different basis sets, different SCF types, different configuration selection thresholds, and/or different CI reference sets for a given H_4 conformation yielded MRD-CI energies that differed systematically, though by relatively small amounts. Extrapolation to zero threshold (performed automatically by the MRD-CI program) and the Davidson correction to full CI are both standard procedures. The London-type basis correction is reasonably well justified, and makes a significant improvement in the accuracy. In addition, we made two small ad hoc corrections, functions of the extrapolation threshold and the SCF type, to improve consistency among the various cases; these latter two corrections were were typically smaller than the random errors in the energies, and could have been omitted with only minor effect on the final energy values.

The Buenker MRD-CI program's extrapolation to zero CI threshold is quite accurate; however, rms differences of 0.42 mE_h remained, between 1753 cases with differing configuration selection thresholds T = 10, 2, or 0.4 μE_h. These rms differences could be reduced to 0.30 mE_h by a small ad hoc systematic correction, described in detail in Appendix B in EPAPS[21]. The rms size of this ad hoc correction was 0.42 mE_h, comparable to the estimated errors in the extrapolation to zero threshold (and smaller than the total estimated MRD-CI errors discussed below).

As in Boothroyd *et al.*[1], we made a parameterized Davidson-type correction to full CI, namely,

$$\Delta_{\mathrm{full-CI}} = \lambda_{DC}^{(\mathrm{SCF})} \Delta E_{DC} = \lambda_{DC}^{(\mathrm{SCF})} (1 - C_R^2) \Delta E_{sd} / C_R^2 \quad , \tag{1}$$

where ΔE_{sd} is the contribution of single and double excitations to the energy, and ΔE_{DC} is the standard Davidson correction. For single-reference closed-shell configurations with at least four electrons, if the effects of quadruple excitations are assumed to be much larger than triple excitations, then the above formula for the Davidson correction (with an expected value of $\lambda_{DC} \sim 0.5$ for closed-shell H_4) can be derived theoretically[30–33]. We not only used multiple references, we also used open and mixed shell SCF cases; we therefore obtained values for the parameter λ_{DC} by minimizing the average differences between MRD-CI energy values

computed for the same point with different reference sets (which thus had different sizes for the Davidson correction). As in Boothroyd *et al.*[1], we used $\lambda_{DC}^{(\mathrm{SCF})} = 0.46$, 0.14, and 0.30 for closed, open, and mixed SCF cases, respectively; the average size of ΔE_{DC} was 1.81, 0.34, and 1.01 mE_h, respectively, yielding full-CI corrections averaging 0.83, 0.05, and 0.30 mE_h, respectively. For 46733 cases where the program obtained improved reference sets, and thus two different-sized Davidson corrections were available, the rms difference between the resulting energies was 0.52 mE_h. This may be an overestimate of the uncertainty, since it may be biased by the rare cases where the larger Davidson correction was very large indeed (up to $\Delta E_{DC} = 18.82$ mE_h). For the 39926 of the above cases where the larger of the resulting ΔE_{DC} was either less than 2.5 mE_h or less than 2.5 times the smaller of the resulting ΔE_{DC}, the rms difference between the resulting energies was 0.31 mE_h. This is probably an underestimate of the uncertainty, as the larger Davidson correction averaged only 1.68 times the smaller one for this latter sample, and there may also be some systematic error since we have no information from cases where only one value of the Davidson correction was available. There are suggestions of a systematic uncertainty of order 0.1 in the preferred value of $\lambda_{DC}^{(\mathrm{SCF})}$, leading to a systematic uncertainty in the energy correction of order 0.2 mE_h. We estimate the total uncertainty in the Davidson-type correction to full-CI to be about 0.5 mE_h.

Small but not completely negligible systematic differences (rms size of 0.55 mE_h) were found in energies computed using molecular orbitals from different SCF types (note that this rms difference gives an estimate of the sum of the "random" errors in extrapolation to zero threshold and the Davidson correction). These rms differences could be reduced to 0.43 mE_h by applying a small ad hoc systematic correction to the relatively few open- and mixed-shell SCF cases. This correction was estimated by comparing MRD-CI energies computed using different SCF types, and is discussed in detail in Appendix B in EPAPS[21]. The rms size of this ad hoc correction was only 0.25 mE_h, much smaller than the estimated MRD-CI errors; and of course it was applied only to those few points where closed-shell SCF was not used.

The final energy value E_{final} was obtained from the estimated full-CI energy using the London-type basis correction described in Boothroyd *et al.*[1]; the average size of this correction was 3.21 mE_h. This London-type basis correction is obtained by taking the difference between the H_4 London energy with the accurate H_2 singlet curve and the H_4 London energy with the H_2 singlet curve computed using the finite basis set:

$$\Delta_{\mathrm{basis}} = V_{London}^{H_4}\{{}^1E_{\mathrm{accurate}}\} - V_{London}^{H_4}\{{}^1E_{\mathrm{basis}}\} \tag{2}$$

The fractional error in this basis correction might be hoped to be of the same order as the fractional error in the London energy. For H_3 geometries, this basis correction has been shown to have an insufficient dependence on the bending angle between the distances r_{12} and r_{23}, and thus for the BKMP2 H_3 surface[22] we added a semi-empirical modification to the H_3 basis correction to alleviate this problem. For H_4, the angular dependence of the London basis correction seems likewise to be insufficient, although there are not enough accurate energies computed with differing basis sets to be certain that this problem is real, and certainly not enough to enable one to attempt any modification of the basis correction. Thus the unmodified London basis correction was used, but our earlier estimate[1] of 0.6 mE_h for the size of its error may be an underestimate: the systematic error in the basis correction

may be closer to 1 mE_h, on average. It will be larger for very compact geometries, and smaller for spread-out geometries (especially those tending towards $H_2 + H_2$).

4. Best MRD-CI energies and estimated errors

The above small corrections reduce but do not completely eliminate inconsistencies in the MRD-CI energies computed with different basis sets, different SCF types, different configuration selection thresholds, and/or different CI reference sets. Where more than one energy value had been computed for a given conformation, the "best" value was chosen to be used in the fitting procedure. (In general, multiple-root cases were preferred to single-root cases, closed shell cases to open and mixed shell cases, lower thresholds to higher ones, and smaller Davidson corrections to larger ones.) The extrapolation to zero threshold and the Davidson-type correction to full CI appear to yield largely "random" errors; the systematic components of these, though not completely negligible, are much smaller than the systematic error in the basis correction. Thus the total uncertainty in the *ab initio* energies probably comprises a "random" error of about 0.5 mE_h and a systematic error of order 1 mE_h.

C. Functional Representation of the H_4 Surface

This section lays out the equations which underlie our fits to the H_4 *ab initio* data. The total H_4 potential energy surface is given by

$$V_{H_4} = V_{London}^{H_4} + V_{nsb}^{H_3} + \sum_{N=1}^{N_{max}} V_N \ , \tag{3}$$

where $V_{London}^{H_4}$ is the London equation for H_4, $V_{nsb}^{H_3}$ is a term based on the non-symmetric bending terms (i.e., non-London terms) from the BKMP2 H_3 surface[22], and the V_N are general H_4 terms used to correct for the deficiencies in the London term ($N_{max} = 8$, except in the earliest of the fits). The separate equations for these terms are given below.

1. The London component

The London component[34], with an added "cusp-rounding" term E_ϵ (as in the BKMP2 H_3 surface[22]), is given by

$$\begin{aligned} V_{London}^{H_4} \ = \ \sum_{i=1}^{6} Q_i - \Big(E_\epsilon^2 + \frac{1}{2}[\,(J_1 + J_6 - J_2 - J_5)^2 \\ +(J_2 + J_5 - J_3 - J_4)^2 + (J_3 + J_4 - J_1 - J_6)^2\,] \Big)^{1/2} \end{aligned} \tag{4}$$

in which

$$Q_i = \frac{1}{2}\left[{}^1E(r_i) + {}^3E(r_i)\right] \quad \text{and} \quad J_i = \frac{1}{2}\left[{}^1E(r_i) - {}^3E(r_i)\right] \tag{5}$$

for each of the six internuclear distances r_i. Note that ${}^1E(r_i)$ is the H_2 singlet energy (obtained from Schwenke's[13] formula), and ${}^3E(r_i)$ is the effective H_2 triplet energy, for one of the six internuclear distances r_i. The effective triplet curve used here was taken unchanged from that used by BKMP2 for their H_3 fit[22]; note that it includes a Johnson[35] correction at small distances to ensure that the difference between the two curves increases monotonically for decreasing values of internuclear separation. As pointed out by Johnson[35], this condition is necessary if one wishes to avoid unphysical discontinuities in the first derivative of the London equation at short distances.

For the BKMP2 H_3 surface[22], a constant value of $E_\epsilon = 1\ \mu E_h$ was used as an (optional) term to slightly round off the cusps in the London equation (e.g., to avoid numerical problems from discontinuous derivatives). However, for the H_4 surface, the London equation inserted cusps in the wrong places (see § III A), and a more general formula was introduced to allow the London cusps to be rounded off by arbitrarily large amounts in certain regions:

$$E_\epsilon(\{r_i\}) = C_{\epsilon E} S^f_\epsilon(\{r_i\}) + (1\mu E_h)[1 - S^f_\epsilon(\{r_i\})] \ , \tag{6}$$

where $C_{\epsilon E}$ is a parameter giving the maximum amount of rounding, and $S^f_\epsilon(\{r_i\})$ is the cusp-rounding switch factor. This switch factor should go to zero for conformations tending towards $H_2 + H_2$ or $H_3 + H$ (since the London component is an essential part of the BKMP2 H_3 surface[22]). If one chooses the "best" way of dividing the H_4 conformation into a separate pair of molecules, the four distances between atoms in separate "molecules" will be large for $H_2 + H_2$, and two of these four distances will be large for $H_3 + H$. Schwenke[13] defined a switch factor $S^{(J)}_g$ to choose between the three ways ($g = 1, 2, 3$) of describing the $H_2 + H_2$ pairing into r_{a_g} and r_{b_g} (AB+CD, AC+BD, or AD+BC); this is discussed in more detail in § II C 3 below: see equation (19). Using this "separate-molecule" switch $S^{(J)}_g$ (a function of r_{a_g}, r_{b_g}, and R_g), we define a "separation measure" s_ϵ as

$$s_\epsilon(\{r_i\}) = \left[\sum_{g=1}^{3} S^{(J)}_g \prod_{i \neq a_g, b_g} (r_i + C_{\epsilon\Delta}) \right]^{1/4} \ , \tag{7}$$

where $C_{\epsilon\Delta}$ is a parameter that reduces the variation among s_ϵ values when the distances r_i are small — in particular, for $H_3 + H$, the sensitivity of s_ϵ to the size of the H_3 sub-conformation is reduced.

Let $C_{\epsilon S}$ be a parameter giving the position in terms of s_ϵ where the London-rounding should be switched on, let $C_{\epsilon W}$ be a parameter giving the half-width of the switch-over region in terms of s_ϵ, and let $\delta_\epsilon = (s_\epsilon - C_{\epsilon S})/C_{\epsilon W}$ (i.e., the fractional separation measure relative to the switchover position); then the cusp-rounding switch factor is defined as

$$S^f_\epsilon(\{r_i\}) = \begin{cases} 1 & , \ \delta_\epsilon \leq -1 \\ 1 - \frac{1}{2}(1 - \delta_\epsilon)^3(1 + \delta_\epsilon) & , \ -1 < \delta_\epsilon < 0 \\ \frac{1}{2}(1 + \delta_\epsilon)^3(1 - \delta_\epsilon) & , \ 0 \leq \delta_\epsilon < 1 \\ 0 & , \ \delta_\epsilon \geq 1 \end{cases} \tag{8}$$

This switch factor has continuous first and second derivatives, and switches smoothly from 1 to 0 as the "separation measure" s_ϵ goes from $C_{\epsilon S} - C_{\epsilon W}$ to $C_{\epsilon S} + C_{\epsilon W}$.

2. Bending terms from the H_3 surface

The term $V_{nsb}^{H_3}$ is based on the non-symmetric bending terms in the BKMP2 H_3 potential[22]. From the four H atoms, there are four possible ways h of choosing 3 atoms (ABC, ABD, ACD, or BCD, corresponding to $h = 1$, 2, 3, or 4, respectively). For each way, we calculate a weighted H_3 term $V_h^{H_3}$, and define

$$V_{nsb}^{H_3} = \sum_{h=1}^{4} V_h^{H_3} \ . \tag{9}$$

The weighted H_3 terms are defined as

$$V_h^{H_3} = S_1(h)\,[V_{asym}(h) + V_{bend}(h)] + S_2(h)\,[C_{all}(h) + C_{asym}(h) + C_{bend}(h)] \tag{10}$$

where the terms V_{asym}, V_{bend}, C_{all}, C_{asym}, and C_{bend} are taken directly from our BKMP2 H_3 surface[22]. The switches (weights) $S_1(h)$ and $S_2(h)$ are defined as follows. For the 3 atoms chosen to be part of the "H_3" (for choice h), call the distances $r_{t1_h}, r_{t2_h}, r_{t3_h}$. Call the other 3 distances $r_{u1_h}, r_{u2_h}, r_{u3_h}$. Let

$$\rho_{t_h} = \left[r_{t1_h}^{-2} + r_{t2_h}^{-2} + r_{t3_h}^{-2}\right]^{1/2} \ , \tag{11}$$

$$\rho_{u_h} = \left[r_{u1_h}^{-2} + r_{u2_h}^{-2} + r_{u3_h}^{-2}\right]^{1/2} \ . \tag{12}$$

The switches (weights) for $V_{nsb}^{H_3}$ are then defined as

$$S_1(h) = [1 + S_1^o \exp(S_1^t/\rho_{t_h} - S_1^u/\rho_{u_h})]^{-1} \ , \tag{13}$$

$$S_2(h) = [1 + S_2^o \exp(S_2^t/\rho_{t_h} - S_2^u/\rho_{u_h})]^{-1} \ , \tag{14}$$

where S_1^o, S_2^o, S_1^t, S_2^t, S_1^u, and S_2^u are six (non-linear) parameters. The combination $V_{London}^{H_4} + V_{nsb}^{H_3}$ asymptotically approaches the BKMP2 H_3 surface[22] as one of the four hydrogen atoms is removed from the vicinity of the other three.

3. General H_4 Jacobi terms

The V_1 term (also referred to as our V_{corr} term, since it is almost identical to the V_{corr} formula of Schwenke[13]), is defined in terms of the Jacobi coordinates $r_a, r_b, R, \theta_a, \theta_b$, and ϕ (strictly, these Jacobi coordinates should also be subscripted by g — see description below):

$$V_1 = e^{-\beta_1 \rho^3} \sum_{g=1}^{3} S_g^{(J)} A_g^{corr}(\{r_i\}) \sum_{q_1 q_2 \mu} \mathcal{Y}_{q_1 q_2 \mu}(\theta_a, \theta_b, \phi) \sum_{i,j=I_{lo}}^{I_{hi}} \sum_{k=K_{lo}}^{K_{hi}} C^{(1)}_{q_1 q_2 \mu, ijk}\, {r_a}^i {r_b}^j R^k \ . \tag{15}$$

Several other similar terms were also introduced, namely V_N for $N = 2$ to N_J:

$$V_N = A_N(\{r_i\})\, e^{-\beta_N \rho^3} \sum_{g=1}^{3} S_g^{(J)} \sum_{q_1 q_2 \mu} \mathcal{Y}_{q_1 q_2 \mu}(\theta_a, \theta_b, \phi) \sum_{i,j=I_{lo}}^{I_{hi}} \sum_{k=K_{lo}}^{K_{hi}} C^{(N)}_{q_1 q_2 \mu, ijk}\, {r_a}^i {r_b}^j R^k \ . \tag{16}$$

Note that the $C^{(N)}_{q_1 q_2 \mu, ijk}$ are the linear parameters of the fitted surface. For most of our fits, we had $N_J = N_{max} = 8$; however, for our final fits (including the final adopted surface), we set $N_J = 7$ and replaced V_8 with a many-body-expansion term based on that used in the Aguado *et al.*[3] surface (see § II C 5).

Each of the general H_4 terms in equations (15) and (16) contains a selector function $A(\{r_i\})$ which is a relatively simple function of the internuclear distances r_i; these are described in § II C 4 below. Each term also contains a factor $e^{-\beta_N \rho^3}$ to reduce the size of the correction for large geometries. Here ρ is a useful measure of the overall size of a given H_4 geometry:

$$\rho = \left[\sum_{i=1}^{6} r_i^2 \right]^{1/2} \quad . \tag{17}$$

In the terms V_1 through V_{N_J}, the description of the H_4 is basically in terms of a pair of H_2 molecules. As in Schwenke[13], we use the Jacobi coordinates r_a, r_b (H_2 molecule sizes), R (intermolecular separation), and the angles θ_a, θ_b, ϕ, where $\phi = \phi_a - \phi_b$. In particular, $\cos\theta_a = \vec{r}_a \cdot \vec{R}/(r_a R)$, $\cos\theta_b = \vec{r}_b \cdot \vec{R}/(r_b R)$, and $\cos\phi = (\vec{r}_a \times \vec{R}) \cdot (\vec{r}_b \times \vec{R})/(|\vec{r}_a \times \vec{R}|\,|\vec{r}_b \times \vec{R}|)$. In addition to the Jacobi coordinates, we also use the six internuclear separations. Here we follow the convention[34] that sets $r_1 = |\vec{r}_{AB}|$, $r_2 = |\vec{r}_{AC}|$, $r_3 = |\vec{r}_{AD}|$, $r_4 = |\vec{r}_{BC}|$, $r_5 = |\vec{r}_{BD}|$, and $r_6 = |\vec{r}_{CD}|$. Since it is not always clear to which distances in the molecule to assign the labels r_a and r_b, we follow Schwenke's[13] method of using all three possible descriptions. For each of the three ways ($g = 1, 2, 3$) of describing the $H_2 + H_2$ pairing (AB+CD, AC+BD or AD+BC), we calculate the following useful quantities in terms of the corresponding Jacobi coordinates r_{a_g}, r_{b_g}, and R_g:

$$\eta_g = \left[(r_{a_g}^{-2} + r_{b_g}^{-2})^{1/2} R_g \right]^{-1} \tag{18}$$

$$S_g^{(J)} = e^{-\beta_J \eta_g} \left(e^{-\beta_J \eta_1} + e^{-\beta_J \eta_2} + e^{-\beta_J \eta_3} \right)^{-1} \quad . \tag{19}$$

Note that $S_g^{(J)}$ is also used in the definition of quantities used in the London cusp-rounding switch of § II C 1 above: see equation (7). The quantities η_g and $S_g^{(J)}$ are used to combine contributions from the three possible descriptions; the smallest value of η_g indicates the best description, and the switch $S_g^{(J)}$ gives the appropriate weight. Schwenke[13] let $\beta_J = 20$ to give rapid switching between the three descriptions. We found that softer switching between the three descriptions resulted in a better fit, and so $\beta_J = 10$ was used in our fit. For some geometries encountered, R_g has a value of zero for at least one of the three descriptions of the best pairing; these situations must be handled as a special case to avoid dividing by zero (note that negative powers of R are possible in the fit). For a case with $R_g < 10^{-15}$ a_0 (or $S_g^{(J)} < 10^{-30}$), the weight for that particular description g was set to exactly zero and the corresponding terms in the fitting formulae were not evaluated.

As in Schwenke's[13] surface, the angular functions are given by

$$\mathcal{Y}_{q_1 q_2 \mu} = \frac{4\pi}{[2(1+\delta_{\mu 0})]^{1/2}} \left[Y_{q_1 \mu}(\theta_a, \phi_a) Y_{q_2, -\mu}(\theta_b, \phi_b) + Y_{q_1, -\mu}(\theta_a, \phi_a) Y_{q_2 \mu}(\theta_b, \phi_b) \right] \tag{20}$$

where $Y_{q,\mu}$ is a spherical harmonic. Due to homonuclear symmetry, only even values of the indices q_1 and q_2 appear in the above equation[13]. The combinations of $q_1 q_2 \mu$ used are

{000, 220, 221, 222, 200, 020}; equations (15) and (16) involve a summation over these combinations. (Note that Schwenke's[13] *ab initio* points did not have general enough symmetry to allow him to determine coefficients for $q_1q_2\mu = 221$, which he therefore omitted in his equations.) The 'radial' dependence in the terms V_1 through V_{N_J} is described by the final summations over i, j, and k in each correction term. Note that the selector functions $A_N(\{r_i\})$ can depend on all six internuclear distances, and are not decomposed into the above 'radial' and 'angular' coordinates.

It is required that the surface be unaffected when r_a is swapped with r_b. This constrains the number of independent $C^{(N)}_{q_1q_2\mu,ijk}$. By symmetry, the range of indices on the summation over the index j must be the same as the range on the summation over the index i. In addition, when doing the triple summations, when $q_1 = q_2$ the off-diagonal elements i, j and j, i must have the same coefficient. This requirement therefore applies to $q_1q_2\mu = 000$, 220, 221, and 222 only. Similarly, the coefficients for $q_1q_2\mu = 200$ are reused as coefficients for the $q_1q_2\mu = 020$ (with ${r_a}^i$ and ${r_b}^j$ changed to ${r_a}^j$ and ${r_b}^i$) to meet the symmetry requirement.

In the general case, given index ranges $n_i = I_{hi} - I_{lo} + 1$ and $n_k = K_{hi} - K_{lo} + 1$, the total number of linear parameters N_{term} for a term with these index ranges may be obtained via

$$\begin{aligned} n_L &= n_k \times n_i \times n_i \\ n'_L &= n_k \times (\textit{no. of elements in upper triangle of } n_i \times n_i \textit{ matrix}) \\ &= n_k \times n_i \times (n_i + 1)/2 \\ N_{term} &= 4 \times n'_L + n_L \end{aligned} \tag{21}$$

Consider an example for any one of the correction terms V_N. If the indices on the triple summation all run from 0 to 2 ($n_i = n_k = 3$), this yields 18 terms for each of $q_1q_2\mu = 000$, 220, 221, and 222 (after adding together the appropriate off-diagonal terms for these four values of $q_1q_2\mu$), and 27 terms for $q_1q_2\mu = 020$, for a total of 99 separate optimizable parameters (not 162 as one would obtain without any of these restrictions imposed by symmetry).

4. Selector functions

Various selector functions $A(\{r_i\})$ were used in an attempt to distinguish certain subsets of the fitted points. The subsets weighted by the various selector functions are not mutually exclusive, but help to reduce the number of linear dependencies between the hundreds of linear terms.

The selector function A^{corr}_g (used in our V_1 term) is a general selector and is based on Schwenke's[13] V_{corr} term; for each of the three possible $H_2 + H_2$ pairings g, with H_2 molecule sizes r_{a_g} and r_{b_g},

$$A^{corr}_g = \sum_{i \neq a_g, b_g} V_p(r_i) \equiv \left[\sum_{i=1}^{6} V_p(r_i) \right] - V_p(r_{a_g}) - V_p(r_{b_g}) \; . \tag{22}$$

As in Schwenke's fit, V_p is the non-bonding pairwise potential

$$V_p(r_i) = \exp\left(-A_{p_2} r_i^{A_{p_3}} \right) \; , \tag{23}$$

containing two non-linear parameters A_{p_2} and A_{p_3}.

The other selector functions $A_N(\{r_i\})$ were defined in terms of all six distances r_i in such a way as to be invariant under interchange of atoms. Recall that under the definition of the r_i (see § II C 3 above), it will always be the case that r_1 and r_6 connect disjoint pairs of atoms, as do r_2 and r_5, or r_3 and r_4. The selector functions were defined as:

$$\begin{aligned} A_2(\{r_i\}) &= A_{kite}(16,23,45) + A_{kite}(61,24,35) + A_{kite}(25,13,46) \\ &\quad + A_{kite}(52,14,36) + A_{kite}(34,12,56) + A_{kite}(43,15,26) \end{aligned} \tag{24}$$

$$A_3(\{r_i\}) = \frac{0.1\,\overline{r}^{\,4}}{0.1\,\overline{r}^{\,2} + A_{tet}(\{r_i\})} + \frac{0.1\,\overline{r}^{\,4}}{0.1\,\overline{r}^{\,2} + A_{sq}(16) + A_{sq}(25) + A_{sq}(34)} \tag{25}$$

$$A_4(\{r_i\}) = A_{H_3H}(124,356) + A_{H_3H}(135,246) + A_{H_3H}(236,145) + A_{H_3H}(456,123) \tag{26}$$

$$A_5(\{r_i\}) = 1.0 \tag{27}$$

$$\begin{aligned} A_6(\{r_i\}) &= \left(\frac{A_{H_3H}(124,356)}{\overline{r}^{\,2}}\right)^6 A_{nonlinH_3}(124) + \left(\frac{A_{H_3H}(135,246)}{\overline{r}^{\,2}}\right)^6 A_{nonlinH_3}(135) \\ &\quad + \left(\frac{A_{H_3H}(236,145)}{\overline{r}^{\,2}}\right)^6 A_{nonlinH_3}(236) + \left(\frac{A_{H_3H}(456,123)}{\overline{r}^{\,2}}\right)^6 A_{nonlinH_3}(456) \end{aligned} \tag{28}$$

$$A_7(\{r_i\}) = A_{H_2H_2}(16,2345) + A_{H_2H_2}(25,1346) + A_{H_2H_2}(34,1256) \tag{29}$$

$$A_8(\{r_i\}) = \sum_{i=1}^{6} A_{compact}(r_i) \tag{30}$$

where

$$\overline{r} = \frac{1}{6}\sum_{i=1}^{6} r_i \tag{31}$$

$$A_{kite}(ij,kl,mn) = \left(\frac{r_i}{r_j}\right)^2 \left(\frac{\overline{r}^{\,2}}{(r_k - r_l)^2 + \overline{r}^{\,2}} + \frac{\overline{r}^{\,2}}{(r_m - r_n)^2 + \overline{r}^{\,2}}\right) \tag{32}$$

$$A_{tet}(\{r_i\}) = \sum_{i=1}^{6} (r_i - \overline{r}\,)^2 \tag{33}$$

$$A_{sq}(ij) = (r_i - r_j)^2 + \overline{r}^{\,2}\left(\frac{r_i + r_j}{\overline{r}} - \frac{6}{2+\sqrt{2}}\right)^2 \left(\frac{r_i + r_j}{\overline{r}} - \frac{6\sqrt{2}}{2+\sqrt{2}}\right)^2 \tag{34}$$

$$A_{H_3H}(ijk,lmn) = \left[(r_i + r_j + r_k) - (r_l + r_m + r_n)\right]^2 \tag{35}$$

$$A_{nonlinH_3}(ijk) = \frac{1}{\overline{r}^{\,4}}(r_i + r_j - r_k)^2 (r_i + r_k - r_j)^2 (r_j + r_k - r_i)^2\,. \tag{36}$$

$$A_{H_2H_2}(ij,klmn) = (r_i - r_j)^2 - (r_k + r_l + r_m + r_n)^2 \tag{37}$$

$$A_{compact}(r_i) = \begin{cases} (r_i - 1.15\ a_0)^3/(r_i - 1.25\ a_0) & ,\ r_i < 1.15\ a_0 \\ 0.0 & ,\ r_i \geq 1.15\ a_0 \end{cases} \tag{38}$$

The selector function A_2 emphasizes "kite-shaped" conformations, A_3 anti-selects against squares and tetrahedra, A_4 distinguishes between "H_3+H" and general H_4 conformations, A_5 is unity (no selection), A_6 is similar to A_4 but selects only non-linear H_3 parts, A_7 distinguishes between "H_2+H_2" and general H_4 conformations, and A_8 selects "compact" conformations containing short distances.

5. General H_4 many-body expansion term

As mentioned in § II C 3, for our final fits (including the final adopted surface) we set $N_J = 7$ (rather than 8) and replaced V_8 with a many-body-expansion term based on that used in the Aguado *et al.*[3] surface:

$$V_8^{(mbe)} = e^{-\beta_8 \rho^3} \sum_{0 \le i,j,k,l,m,n \le L_{hi}}^{\substack{i+j+k+l+m+n \\ \le M_{order}}} C^{(8)}_{ijklmn} \sum_{\substack{\text{permutations} \\ \text{of H atoms}}} p_1^i \, p_2^j \, p_3^k \, p_4^l \, p_5^m \, p_6^n \ , \tag{39}$$

where $C^{(8)}_{ijklmn}$ are the linear parameters, and the polynomial Rydberg-type variables[3,36] p_ν are simple functions of the corresponding internuclear distances r_ν, for $\nu = 1$ to 6:

$$p_\nu = r_\nu \, e^{-\beta_p \, r_\nu} \ , \tag{40}$$

with a non-linear parameter β_p. The sum of the six indices must never exceed M_{order}, the order of the surface; in addition, we constrained the maximum power for any individual distance by requiring that no index exceed a limit L_{hi}. (Note that our choice of numbering the distances r_ν differs from that of Aguado *et al.*[3]; their notation is recovered by exchanging r_3 with r_4, or indices k with l. The four-body term of Aguado *et al.*[3] is then obtained by setting $\beta_8 = 0.0$ and $L_{hi} = M_{order}$.)

As pointed out by Aguado *et al.*[3], some constraints on the indices are needed to make sure that this is indeed a four-body term, i.e., that for each way of dividing H_4 into two or more disjoint subsets, the disjoint subsets are always connected by at least one distance with a non-zero index. This can be accomplished by the two conditions that (i) each H atom must have at least one distance with a non-zero index:

$$i + j + k > 0 \ , \quad i + l + m > 0 \ , \quad j + l + n > 0 \ , \quad k + m + n > 0 \ , \tag{41}$$

and (ii) at least three of the six indices are non-zero:

$$\min\{i,1\} + \min\{j,1\} + \min\{k,1\} + \min\{l,1\} + \min\{m,1\} + \min\{n,1\} \ge 3 \ . \tag{42}$$

[This latter is the condition that the next-to-last line in equation (6) from Aguado *et al.*[3] was *intended* to express, although their equation (6) actually allowed up to four indices to be zero, provided that the remaining two indices were 2 or higher — the correct conditions were embedded in their fitted surface, however.]

The requirement that the surface be symmetric under interchange of H atoms is met in equation (39) by the sum over all 4! permutations of the H atoms. Given this symmetrization sum, further conditions on the indices are required to avoid duplicate terms. These conditions may be expressed as:

$$\begin{gathered} i \ge j \ge k \ , \quad j \ge l \ , \quad j \ge m \ , \quad i \ge n \ , \qquad \text{if } i = j \text{ then } m \ge n \ , \\ \text{if } j = k \text{ then } l \ge m \ , \qquad \text{if } j = l \text{ then } k \ge m \ , \\ \text{if } j = m \text{ or } i = n \text{ then } k \ge l \ , \qquad \text{if } i = l \text{ then } k \ge n \ . \end{gathered} \tag{43}$$

Combining all of the above conditions, the sum over indices then yields all different symmetry adapted functions for the relevant four-body terms of H_4. If, for example, one sets $L_{hi} = 3$

and $M_{order} = 8$, then one obtains 95 independent linear parameters $C^{(8)}_{ijklmn}$ (as opposed to 99 linear parameters in a V_N term, with $N \leq N_J$, having $I_{hi} = K_{hi} = 2$ and $I_{lo} = K_{lo} = 0$). Aguado *et al.*[3] set $L_{hi} = M_{order} = 12$ in their best-fit surface, for a total of 865 linear parameters.

6. Other types of terms tested

Many different versions were tried for the selector functions of § II C 4 before the final versions given above were decided upon, and many different summation index ranges and different subsets of the above terms V_N were tested. A lower-powered cutoff factor $e^{-\beta\,\rho^2}$ (rather than $e^{-\beta\,\rho^3}$) was tried in equations (15) and (16), but was found to yield a poorer fit. Likewise, an alternate cutoff factor $e^{-\beta\,\overline{r}^{\,n}}$ was tested, using the mean internuclear separation $\overline{r}$ (to some power n) instead of the rms internuclear separation ρ [see equations (31) and (17)]. A switch to turn off the entire London term of equation (4) was tried, in place of the switch to turn on London cusp-rounding [equations (6) through (8)]. In addition, two entirely different types of terms were tried in the H_4 surface.

A term V_{sym} was tested, of a form similar to the many-body-expansion term but of higher symmetry, being symmetric under all 6! permutations of the interatomic distances (rather than the 4! permutations of the H atoms):

$$V_{sym} = A_{sym}(\{r_i\})\, e^{-\beta_s\,\rho^3} \sum_{\substack{0\leq i\leq j\leq k\leq l \\ \leq m\leq n\leq L_{hi}}}^{\substack{i+j+k+l+m+n \\ \leq M_{order}}} C^{(s)}_{ijklmn} \sum_{\substack{\text{permutations} \\ \text{of (123456)}}} p_1^i\, p_2^j\, p_3^k\, p_4^l\, p_5^m\, p_6^n\ , \tag{44}$$

where no more than two of the powers $\{i, j, k, l, m, n\}$ were allowed to be zero for any term in the summation. A selector function of $A_{sym}(\{r_i\}) = 1$ (no selection) was the most obvious choice to try, but other possibilities were tested as well.

With $L_{hi} = 4$ and $M_{order} = 13$, this term V_{sym} contains 95 linear parameters to be fitted, as opposed to 99 linear parameters in a V_N term with $I_{hi} = K_{hi} = 2$, $I_{lo} = K_{lo} = 0$. However, replacing one such V_N term with V_{sym} not only increased the CPU-time required for surface evaluation by a large factor, it was also significantly less effective: it led to an increase of about 15% in the rms error of the fitted *ab initio* energies (in a fit with a total of about 790 parameters). Moreover, the high powers of the interatomic distances (introduced in order to obtain a significant number of distinct terms in V_{sym}) would tend to introduce unphysical "wiggles" in the fitted surface. The term V_{sym} was therefore abandoned.

A V_{H_3H} term was also tried, using some of the quantities defined for $V^{H_3}_{nsb}$ in § II C 2:

$$V_{H_3H} = A^{(H_3H)}(\{r_i\})\, e^{-\beta_H\,\rho^3} \sum_{h=1}^{4} S_1(h) \sum_{i=I_{lo}}^{I_{hi}} \sum_{k=K_{lo}}^{K_{hi}} C^{(H_3H)}_{ik}\, \mathcal{R}^i_{t_h}\, \mathcal{R}^k_{u_h} \tag{45}$$

where as selector functions we tried both $A^{(H_3H)}(\{r_i\}) = A_3(\{r_i\})$ and $A^{(H_3H)}(\{r_i\}) = \overline{r}^{\,4}/[0.1\,\overline{r}^{\,2} + A_3(\{r_i\})]$ [see equations (26) and (31)], and as "distance values" $\mathcal{R}$ we tried both $\{\mathcal{R}_{t_h} = r_{t1_h} + r_{t2_h} + r_{t3_h}, \mathcal{R}_{u_h} = r_{u1_h} + r_{u2_h} + r_{u3_h}\}$ and $\{\mathcal{R}_{t_h} = r_{t1_h} r_{t2_h} r_{t3_h}, \mathcal{R}_{u_h} = r_{u1_h} r_{u2_h} r_{u3_h}\}$ [see equations (11), (12), and (13)]. Like V_{sym}, the V_{H_3H} term proved much less useful than the V_N terms, and was discarded.

D. Our Approach to Fitting

This section outlines in general the steps followed in developing the terms and optimizing the parameters in our analytical representation of the H_4 surface. The details of the equations are given in § II C above.

We started with the London H_4 equation, with the negligible cusp-rounding $E_\epsilon = 1\ \mu E_h$ (see § II C 1). As described in Boothroyd *et al.*[1], we found that it fit our set of H_4 *ab initio* energies about as well as any of the H_4 surfaces existing at that time (though the subsequent Aguado *et al.*[3] surface of course did much better). Since the parameters in the London equation are fixed, other terms in the fit were added to correct for differences between the London representation and the data. After discovering that, unlike H_3, the cusps in the London H_4 equation did not correspond well with the position of the conical intersection with the first excited state, E_ϵ was modified to allow non-negligible cusp-rounding as a function of the internuclear distances: see equations (6) and (7) in § II C 1.

To compare the quality of different fits numerically, we monitored the rms values of various subsets of the points after the completion of each fit. The following subsets were monitored: (a) all 61547 points, (b) all 48180 *ab initio* points, (c) the 2500 $H_4 \rightarrow H_3 + H$ *ab initio* points (these include one of Schwenke's points), (d) the 8559 H_4fromH_3 points, (e) the 10 *ab initio* tetrahedra, (f) the 11 *ab initio* squares, (g) the 1197 H_4London points, and (h) the 3611 S&K-H_2+H_2 points. Once a small number of "good" fits had been selected numerically, various subdivisions of the above subsets were considered, and a large number of graphs and contour plots were used to select the surface that appeared to have the fewest non-physical "wiggles".

1. Weights applied to fitted energies

In this section, the weights referred to are those that were used to multiply the deviations between the fit and the data, before squaring these weighted deviations to calculate the rms of the fit. Note that, frequently, the "weight" in a fit is defined as that applied to the square of the (unweighted) deviation, i.e., with this definition the weight would be the *square* of the values reported below.

Several different criteria were used to determine weight values. If more than one applied, the final combined weight used was the *product* of the individual weight factors from the following separate criteria.

Higher *ab initio* energies have larger uncertainties than lower energies, and high-energy portions of the surface are less likely to be accessed in collisions of hydrogen molecules. Thus *all* points with high energy E were given reduced weight, namely,

$$w_E = \begin{cases} 1 & , \ E \leq 0.2\ E_h \\ (0.2\ E_h)/E & , \ E > 0.2\ E_h \end{cases} \tag{46}$$

i.e., a weight inversely proportional to the energy for cases with energies more than about 3.1 times the H_2 dissociation energy above that of a pair of separated equilibrium H_2 molecules.

The generated Schaefer & Köhler $H_2 + H_2$ points (see § II A 6) should be of high accuracy for near-equilibrium H_2 molecule sizes; they lie in or near the van der Waals well, which has

a depth of order 0.1 mE_h. Their absolute accuracy will be less in the repulsive wall inside the van der Waals well, or for the cases that we generated with non-equilibrium H_2 molecule sizes. For Schaefer & Köhler $H_2 + H_2$ points *only*, two weight factors w_r and w_R were combined, the former depending on the H_2 sizes r_a and r_b, and the latter on a modified intermolecular separation R':

$$w_r = \begin{cases} 80 \ , & r_a = r_b = 1.449\ a_0 \\ 60 \ , & \text{else if } 1.2\ a_0 \le \{r_a, r_b\} \le 1.75\ a_0 \\ 30 \ , & \text{else if } 1.0\ a_0 \le \{r_a, r_b\} \le 2.1\ a_0 \\ 20 \ , & \text{else if } 0.8\ a_0 \le \{r_a, r_b\} \le 2.6\ a_0 \\ 10 \ , & \text{otherwise: i.e., } \min\{r_a, r_b\} = 0.6\ a_0 \text{ or } \max\{r_a, r_b\} = 3.4\ a_0 \end{cases} \tag{47}$$

$$w_R = \begin{cases} 0.11 \ , & R' < 4.6\ a_0 \\ 0.333 \ , & 4.6\ a_0 \le R' < 5.4\ a_0 \\ 1.0 \ , & 5.4\ a_0 \le R' < 5.9\ a_0 \\ 3.0 \ , & 5.9\ a_0 \le R' < 8.9\ a_0 \\ 4.0 \ , & R' \ge 8.9\ a_0 \end{cases} \tag{48}$$

where

$$R' = R - |\cos\theta_a| \max\left\{\frac{r_a - 1.5\ a_0}{2}, 0.0\ a_0\right\} - |\cos\theta_b| \max\left\{\frac{r_b - 1.5\ a_0}{2}, 0.0\ a_0\right\} \tag{49}$$

i.e., R' is reduced relative to R by the the extent to which the ends of larger-than-equilibrium H_2 molecules are closer to each other than equilibrium H_2 molecules would be (ignoring their relative orientation ϕ around the axis joining the H_2 molecules).

The "H_4fromH_3" points generated from both the *ab initio* and the generated H_3 points (see § II A 8) are of higher accuracy than the H_4 *ab initio* points, and the BKMP2 surface (to which the fitted H_4 surface should reduce for such conformations) fits the *ab initio* H_3 points to an rms (unweighted) accuracy of 0.27 mE_h, and the generated $H_2 + H$ points even better[22]. These points were thus assigned an increased weight of $w_3 = 10$.

The very compact "H_4London" points generated from the London equation (see § II A 7) are of very low accuracy, and were intended only to provide a rough guide to the surface extrapolation to small distances and high energies. These points were thus assigned a reduced weight of $w_L = 0.05$.

2. Optimization of non-linear parameters

In the A^{corr} selector function of equation (22) for the V_1 (i.e., V_{corr}) term of the surface [equation (15)], there are two non-linear parameters A_{p_2} and A_{p_3}. There are two H_3 switches involving a total of six non-linear parameters [see equations (13) and (14)] — these switches control the switchover to the BKMP2 H_3 surface[22] as one hydrogen atom is removed to a large distance from the other three. These eight parameters were varied using a nonlinear fitting procedure. At this point, only the terms $V^{H_4}_{London}$ (with $E_\epsilon = 1\ \mu E_h$), $V^{H_3}_{nsb}$, and $V_1 \equiv V_{corr}$ were included in the fit: see equations (3), (4), (9), and (15). Limits of $(I_{lo}, I_{hi}) = (K_{lo}, K_{hi}) = (-1, 2)$ were used in the ijk summations of equation (15) at this point, yielding a total of 224 linear parameters. The points fitted at this time included only the original

6101 *ab initio* H_4 energies, the 3611 "$H_2 + H_2$" points, the 1194 "H_4London" points, and a subset of 891 "H_4fromH_3" points. At each cycle of the nonlinear least squares optimization, the 224-parameter linear least squares problem was solved anew. The resulting rms error for the 6101 *ab initio* energies was 4.0 mE_h. Once converged, these parameters for A^{corr} and the H_3 switches were left constant for the remainder of the fits.

Additional non-linear parameters β_N (for $N = 1, \ldots, N_{max}$) appear in the exponential cutoff terms $e^{-\beta\rho^3}$ in equations (15), (16), and (39). These were not fitted, but a number of different β values were tested, and final values chosen such that the van der Waals well had enough flexibility to be fitted reasonably but not so much that "wiggles" appeared there (or beyond). Different powers of ρ in the exponential were also tested; ρ^3 worked best. The same value was used for most of the β_N, but a lower value was used for β_6, since the corresponding selector function A_6 selects conformations tending towards non-linear $H_3 + H$, and our *ab initio* energies indicate that the fourth H atom has a non-negligible interaction energy with the non-linear H_3 out to larger distances than is the case for $H_2 + H_2$. There was one case where a β value was indeed fitted: in the final fits, when the compact-term V_8 was replaced by the many-body-expansion term $V_8^{(mbe)}$, the parameter β_8 was varied along with two other non-linear parameters, β_p [see equations (39) and (40) in § II C 5], and $C_{\epsilon E}$ [see equation (6) in § II C 1].

In the London cusp-rounding E_ϵ of equation (6), there are four non-linear parameters $C_{\epsilon\Delta}$, $C_{\epsilon S}$, $C_{\epsilon W}$, and $C_{\epsilon E}$. The first of these, $C_{\epsilon\Delta}$, is used in the the definition of the "separation measure" s_ϵ to reduce the sensitivity to H_3 size in $H_3 + H$ conformations; a value of $C_{\epsilon\Delta} = 3.0\ a_0$ was chosen, that provided a reasonable separation between "H_4fromH_3" conformations and conformations of the worst-fitted points (from best of the fits that did *not* include cusp-rounding). The position $C_{\epsilon S}$ and half-width $C_{\epsilon W}$ of the switch (in terms of s_ϵ) were not varied continuously; rather, several dozen different cases with different positions and widths were tested. For each of these cases, the optimum amount $C_{\epsilon E}$ of rounding was determined by performing a non-linear optimization minimizing the (energy-weighted) rms error of the 48180 *ab initio* H_4 points; this H_4 *ab initio* rms error for each test value of $C_{\epsilon E}$ was obtained by performing a linear fit for the *full* set of equations fitted (with the full weights of § II D 1) to *all* 61547 conformations (both *ab initio* and non-*ab initio*).

The values of all the above non-linear parameters are given in Table I, including the London cusp-rounding parameters for the six "best" fits, which we have labelled surfaces "F", "E", "D", "C", "B", and "A" — in the last two of these, the compact-term V_8 was replaced with the many-body-expansion term $V_8^{(mbe)}$. Note that surface "G" is the best fitted surface *without* any London cusp-rounding. The adopted surface "Ad" is a version of surface "A", with a reduced number of parameters, as discussed in § II D 4 and III B below.

3. Direct solution for n linear parameters

In performing the simultaneous determination of the hundreds of coefficients in the seven linear correction terms, a matrix, $\mathbf{F}$, which was m points by n linear terms was constructed (in this case, up to about 12000 by 1200 for the original fits, and 70000 by 1200 for the later ones ... quite a large matrix). The i, j element of $\mathbf{F}$, is the j-th linear correction term evaluated using the i-th geometry and energy (where the energy has already been corrected by

other terms not currently being optimized, i.e. the London energy and the V_{H_3H} correction). After constructing the matrix, the eight 'blocks' of $\mathbf{F}$ (one for each of the eight correction terms) were then each rescaled separately using the block average value so that the average in each block was 0.1. This rescaling was done for increased numerical stability during the inversion step. The next step was to calculate $\mathbf{F}^\dagger\mathbf{F}$ to obtain an n by n matrix, $\mathbf{Q}$. This step involved the computation of hundreds of thousands of vector dot products where each vector has a length of about 70000. The resulting matrix, $\mathbf{Q}$, was then inverted numerically to obtain the solution to the linear least squares problem. To accomplish this inversion, the subroutine INVERT was used (originally part of program MINVRD from the University of Toronto FORTRAN library). This inversion procedure performs pivots around the largest element in each row for the maximum numerical stability. This routine was modified slightly so that if it encountered a term that was linearly dependent on some previous term (or combination of terms), it would simply give the dependent term a coefficient of zero and continue with the inversion, instead of aborting. Normally, in a fit of several hundred linear parameters, a few linearly dependent terms were found (up to a few dozen, for fits with larger index ranges), and between 10 and 20% of the terms were found to be essentially "useless" (i.e., with the formal error for the fitted parameter being larger than the fitted parameter value).

4. Elimination of insignificant terms

After deciding on a final form for the fitting functions, the inversion process was repeated, this time adding in one coefficient at a time, in order, from the most significant to the least significant. Adding the most significant term at each iteration automatically avoids the problem of linearly dependent terms. This method of solving for the coefficients was done using the program 'STEPWISE' (written by M. R. Peterson of the Department of Chemistry at the University of Toronto, who adapted it from 'Procedure STEPWISE' by G. H. Goodnight of SAS Institute, N.C., U.S.A.).

The STEPWISE method gives a very slightly better final rms value than the INVERT method (better by of order 1 μE_h). This difference is understandable since the two methods are somewhat different. STEPWISE chooses the next best term at each step, and even compares terms already 'in' to see if swapping some terms 'in' or 'out' might help the rms value.

For the development of our fit "A", Figure 1 shows the stepwise reduction in the weighted rms value as more linear parameters are added to the fit, one by one; energy-weighted rms values for subsets of the *ab initio* H_4 points are also shown at every 50^{th} step. The adopted fit "Ad" corresponds to $N_{step} = 400$ on this plot. The rms values of the other "best" fits followed very similar trends as a function of the number of linear parameters. Keeping about half of the terms for these surfaces is enough to yield a weighted rms only a few percent higher than one would get if the entire matrix were inverted.

E. Re-Fitting The Aguado Surface

By replacing the terms $V_{London}^{H_4}$ and $V_{nsb}^{H_3}$ in equation (3) with the H_3/H_2 terms of Aguado *et al.*[3], eliminating all the V_N terms except for $V_8^{(mbe)}$ [from equation (39)] with $L_{hi} = M_{order} = 12$, and setting $\beta_8 = 0.0$, we were able to attempt to refit the surface of Aguado *et al.*[3]. This surface has one non-linear parameter β_p and 865 linear parameters. We tried three cases: "ASPo", refitting only the original 6101 *ab initio* energies, similar to the fit of Aguado *et al.*[3] (though with corrected energy values in a few cases: see § II B); "ASPa", refitting all 48180 *ab initio* energies; and "ASPf", refitting the full set of 61547 energies.

Unfortunately, due to the large number of terms with high powers, the resulting correlation matrix **Q** proved inadequate for the Aguado *et al.*[3] surface: the matrix inversion step yielded rms values of order 50 mE_h, and even STEPWISE reported "no further improvement possible" at an rms of ~ 3 mE_h, after only about half of the terms had been selected. For surfaces "ASPo" and 'ASPa", the best rms error was obtained by simply *refining* the Aguado *et al.*[3] surface, i.e., retaining $\beta_p = 1.404$ ${a_0}^{-1}$ and fitting the residuals when the Aguado *et al.*[3] surface was subtracted from the *ab initio* points (and thus obtaining refined values for about half of the linear parameters). For surface "ASPf", a good fit in the high-weight van der Waals region required a lower value for β_p, and a straightforward fit to the full set of points did best.

It is possible to estimate the extent to which the refitted many-body expansion surfaces could be improved if an optimal set of parameters was actually attained. For surface "ASPo" (fitted to the 6101 old *ab initio* energies), a straightforward fit yielded an (energy-weighted) rms of 3.06 mE_h with 356 linear parameters and an optimized value of the non-linear parameter $\beta_p = 1.36$ ${a_0}^{-1}$. With the Aguado *et al.* value of $\beta_p = 1.404$ ${a_0}^{-1}$, a straightforward fit yielded only a slightly worse rms of 3.09 mE_h (with 367 linear parameters); the original Aguado *et al.*[3] surface had an rms of 1.95 mE_h, and our differential-Aguado fit (with refined values for 365 parameters) yielded an improved rms of 1.79 mE_h. For surface "ASPa" (fitted to all 48180 *ab initio* energies), a straightforward fit yielded an rms of 3.03 mE_h with 342 linear parameters and a value of $\beta_p = 1.30$ ${a_0}^{-1}$; with $\beta_p = 1.404$ ${a_0}^{-1}$, a straightforward fit yielded only a slightly worse rms of 3.19 mE_h (with 372 linear parameters), and our differential-Aguado fit (with refined values for 370 parameters) yielded an improved rms of 2.61 mE_h. This suggests that, even without trying to fit the van der Waals well, a many-body expansion surface such as that of Aguado *et al.*[3] cannot be expected to fit the *ab initio* energies to better than ~ 2 mE_h. Adding the Schaefer & Köhler van der Waals energies to the points to be fitted can only worsen the fit to the *ab initio* energies. Since the best of the fitted surfaces of the current work have an rms error of ~ 1 mE_h for the *ab initio* energies (a factor of 2 better — they also fit the van der Waals well about 4 times better than the best of the refitted Aguado surfaces), it did not seem worthwhile to expend a large amount of effort to get a relatively minor improvement in a large many-body expansion surface, especially given the fact that the high powers of the distance factors in the expansion might yield short-range wiggles in the analytic surface.

III. DISCUSSION

Table II compares the rms errors of three earlier analytic H_4 surfaces and nine fitted surfaces of this work, for various subsets of *ab initio* and generated energies. "Energy-weighted" deviations were used to obtain these rms values, i.e., energies above about three H_2-dissociation energies were given reduced weight according to the formula of equation (46). The only exception to this is the last line of Table II, where the *fully weighted* rms values of *all points* in our H_4 fit is reported (this is the rms value that the fitting programs described in § II D 3 and II D 4 tried to minimize).

Among the subsets of "all *ab initio* H_4", the "$E < 0.0\ E_h$" and "$E < -0.174\ E_h$" subsets exclude points with *ab initio* energies above two and one dissociation energies, respectively (relative to a pair of separated H_2 molecules). Subsets such as "$A \geq 1.15\ a_0$" refer to non-compact conformations of H_4, since "A" is the shortest of the six interatomic distances (as in § II A). The selector "$t < 3.5$" yields conformations tending towards $H_2 + H_2$. The "random H_4" subset refers to the randomly-generated conformations described in § II A 4. The "original H_4" subset refers to the recomputed versions of the *ab initio* energies of Boothroyd *et al.*[1]; note that, for all but 9 of the points, the new *ab initio* energies agree with the old ones, within the uncertainties. The "Schwenke's H_4" subset refers to the *ab initio* energies of Schwenke[13,14], most of which tend towards $H_2 + H_2$. There are only a few "tetrahedra" and "squares"; they tend to lie at high energies, on or near the conical intersection with the first excited state, and are included here mainly because they were among the subsets kept track of during the fitting process. The "$H_4 \rightarrow H_3 + H$" subset refers to *ab initio* energies of conformations where the fourth H atom lies at some distance from the other three, but where the interaction energy between the H_3 and the fourth H atom is still reasonably large; most of these cases come from the grid described in § II A 2. The "S&K $H_2 + H_2$" subset contains the energies described in § II A 6, generated from a version of the Schaefer and Köhler[9] rigid-rotor $H_2 + H_2$ surface with modifications to allow non-equilibrium H_2 sizes; these generated energies are expected to be most accurate in the equilibrium-H_2 van der Waals well, i.e., the subset with H_2 molecule sizes $r_a = r_b = 1.449\ a_0$ and intermolecular separation $R \geq 5.9\ a_0$. The "H_4fromH_3" subset refers to the H_3 conformations of BKMP2[22] with a fourth H atom added randomly at a large distance, as described in § II A 8. The "cusp-test H_4" subset was *not* included in the fit; as discussed in § II A 5 and III A, these points were used to map out the conical intersection between the ground state and the first excited state, and the rms error of this subset gives an estimate of the extent to which the fitted surfaces fail to reproduce the cusp at this conical intersection.

Three previously-existing H_4 surfaces are shown in Table II. Surface "Th" is the H_4 surface of Keogh[2], having a form somewhat similar to the surfaces of the present work but with some undesirable features (including much larger spurious wiggles for somewhat compact conformations); it was fitted to the original 6101 *ab initio* energies of Boothroyd *et al.*[1], plus the $H_2 + H_2$ van der Waals energies and a subset of the "H_4fromH_3" energies. Surface "Tr" is a slightly improved version of surface "Th" (fitted to the same set of energies); it was used for some semi-classical trajectory calculations by Martin *et al.*[4] and Mandy *et al.*[5]. Surface "ASP" is the many-body expansion H_4 surface of Aguado *et al.*[3], which was fitted only to the original 6101 *ab initio* energies. Of these three, the "ASP" surface does least well on overall H_4 *ab initio* energies, and in addition has spurious wiggles of order 1 mE_h in the

van der Waals region (an order of magnitude larger than the errors of the "Th" and "Tr" surfaces there), but has the smallest spurious wiggles for relatively compact H_4 geometries. Even for the restricted subset of energies to which these three earlier surfaces were fitted, the best surfaces of the current work yield a significant improvement.

As discussed in § II E, the particular form of the Aguado *et al.*[3] many-body expansion surface made it difficult to refit: even the best of our refits have optimized values for less than half of the linear parameters, and even these may still be slightly sub-optimal due to the numerical problems. Table II displays surface "ASPo" (a differential refit to the 6101 original *ab initio* energies, yielding refined values for 365 of the 865 linear parameters and keeping Aguado's values for the other 500), surface "ASPa" (a differential refit to all 48180 *ab initio* energies, yielding refined values for 370 of the 865 linear parameters), and a full H_4 fit "ASPf" (refitting the full set of 61547 energies, using 351 linear parameters plus the non-linear parameter β_p: see Table I). As detailed in § II E, it seems likely that even a "perfect" refit of the Aguado *et al.*[3] surface would still be a factor of 2 worse than the best surfaces of the current work. (In this regard, it should be noted that, for our best surfaces, obtaining optimized values for only half of the linear parameters still brought the rms error to within 5% of its value with *all* parameters optimized.)

Of the other surfaces from the present work displayed in Table II, surface "G" is the best fit that does not include London cusp-rounding (see § II C 1); the presence of the London component in this fitted surface often produces cusps in regions where there is in fact no conical intersection with the first excited state, and frequently fails to predict a cusp where the conical intersection actually occurs (the conical intersection with the first excited state is discussed in more detail below). Four fits ("F", "E", "D", and "C"), with four different London cusp-rounding regimes (see Table I) but otherwise similar to surface "G", have similar rms errors, but are in all cases an improvement on surface "G"; of these four, only the best two ("F" and "C") are displayed in Table II.

The surfaces "B" and "A" have much the same functional form as "F" and "C", respectively; the main difference is that a 99-parameter term V_8 (that selected only geometries with compact distances $< 1.15\ a_0$) was replaced with a 95-parameter many-body expansion term $V_8^{(mbe)}$ (this term is of relatively low order in the distance factors p_ν, unlike the Aguado *et al.*[3] H_4 surface: see § II C 5). Since surfaces "B" and "A" have very similar rms values, only the slightly better of the two ("A") is displayed in Table II. There is only a slight overall improvement relative to surface "C", but in one region there is a *major* improvement: the added flexibility (due to the many-body expansion term) yields a factor of 5 improvement in the fit to the van der Waals well.

Given several surfaces with very similar rms errors, the main criterion for preferring one surface over another was the extent of spurious wiggles in the surface. Hundreds of plots of the seven surfaces "G" through "A" were examined, with surfaces "C" and "A" appearing to be the best in this respect. A further reduction in spurious wiggles could be achieved by keeping only the most effective terms in the surface, at a slight cost to the rms error. For the six best surfaces "F" through "A", reduced-parameter versions were obtained, where the STEPWISE fitting program was instructed to keep only the most significant 400 linear parameters (see § II D 4). Table II displays rms values for "Cd" and "Ad" (reduced-parameter versions of surfaces "C" and "A", respectively). The adopted surface "Ad" has

only slightly higher rms errors than surface "A", and appears to yield the best compromise between goodness of fit and lack of spurious wiggles.

In the following subsections, we discuss in more detail some of the concerns mentioned above, and consider the quality of the fit in various regions of H_4 conformation space.

A. Conical intersection with first excited state

Since our highest-symmetry *ab initio* points were among the first ones to be computed with multiple roots, it soon became clear that the ground state and the first excited state were degenerate for most equilateral-pyramid conformations (three atoms in an equilateral triangle, with the fourth atom directly above the center — C_{3v} symmetry). Shifting the position of the fourth atom from the center-line of the equilateral base, or distorting the shape of the base, lifts the degeneracy. The H_4 London equation exhibits a cusp as one passes through an equilateral-pyramid geometry, just as the H_3 London equation has a cusp at the conical intersection equilateral-triangle H_3 conformations. Another similarity between H_4 and H_3 is an "anomaly" at small sizes. Multiple-root *ab initio* energies computed at compact geometries for the BKMP2 H_3 PES[22] demonstrated that sufficiently small equilateral triangles ceased to represent conical intersections of the H_3 ground and excited states (the non-degenerate A_1' root dips below the degenerate E' roots at small sizes). In the H_4 surface, for equilateral pyramids with base sizes smaller than 2 a_0, a similar thing happens for pyramid heights of ~ 3 a_0; the range of pyramid heights where this happens grows larger with decreasing pyramid base size (see Appendix C in EPAPS[21]).

In contrast to the H_3 surface, for the H_4 surface the conical intersection between ground state and first excited state is by no means confined to conformations with C_{3v} symmetry. When we looked at the worst points in one of our earlier fits, we found that many of them were on or near conical intersections. However, in general the London equation either had a cusp nearby but in the wrong position, or had no cusp in the vicinity at all. Not only did this lead to geometries with large errors, but the other terms in the fit were frequently trying to "flatten out" a spurious cusp as much as possible, or add a "bump" to approximate an absent cusp.

We went to some effort to map out the positions of the conical intersection, in the hopes that it might be simple enough to incorporate into the fitted surface. Unfortunately, the conical intersection turns out to lie on a rather complicated 3-dimensional hypersurface in the 6-dimensional conformation space of H_4. Mapping out a reasonable portion of the conical intersection required computation of 13356 *ab initio* points (with multiple roots); this is described in detail in Appendix C in EPAPS[21]. Even this yielded only a partial characterization; obtaining a *full* characterization is beyond the scope of this paper.

Given the complexity of the geometry of the conical intersection, and the possibility of unexpected behavior at relatively small distances, it was decided that any attempt to include the conical intersection explicitly in our H_4 surface fit would be pointless. Instead, we included a factor in the London component of the fit to round off the London cusps for H_4 conformations (see § II C 1). This led to somewhat smaller errors in the region of the conical intersection (and of the spurious London cusps) and improved the overall rms error significantly.

There are two methods by which one can estimate the fraction of the 6-dimensional H_4 conformation space affected significantly by the conical intersection. The first method is to consider the fraction of the "random" H_4 *ab initio* energies that are poorly fitted by the adopted surface, e.g., with errors more than about 4 times the rms surface error of 0.99 mE_h for this subset. This yields a fraction between 0.1% and 1%, but this method can be criticized on the basis that the "random" H_4 subset was distributed quite non-uniformly in conformation space. The alternative method is to consider that the conical intersection comprises a 3-dimensional hypersurface in the 6-dimensional H_4 conformation space. The width in the other 3 dimensions over which the conical intersection causes the *ab initio* energies to differ significantly from a smooth fitted surface appears to be typically $0.5 - 1.0\ a_0$, as opposed to a range of order $5\ a_0$ where interaction energies are significant. Taking the cube of the ratio of these two width estimates, one again obtains a fraction between 0.1% and 1% of H_4 conformation space to be significantly affected by the conical intersection. It should also be noted that the conical intersection can only be reached when the total $H_2 + H_2$ energy is greater than the H_2 dissociation energy.

Given the relatively small volume of the 6-dimensional H_4 conformation space affected significantly by the conical intersection, the 13356 *ab initio* energies computed to map it out were *not* included in any of the surface fits of the present work. The presence of such a large number of *ab initio* points in such a small fraction of the volume would skew the fitted surface towards an improved fit near the conical intersection, at the expense of a much worse fit over the major portion of the H_4 conformation space.

B. The adopted fit

In addition to varying the non-linear parameters as described above in § II D 2, various functions were tried for the selector functions (the final forms being those described in § II C 4), and various ranges were tested for the ijk indices in equations (15) and (16) in § II C 3. For the same number of linear coefficients, use of negative indices gave a better fit for compact conformations but a poorer fit for more typical conformations. Larger index ranges (i.e., more linear coefficients) produced a more accurate fit, but increased the size of non-physical "wiggles" in the surface. In the end, index ranges $(I_{lo}, I_{hi}) = (K_{lo}, K_{hi}) = (0, 2)$ were used, yielding a reasonable compromise between accuracy and smoothness. For the many-body expansion term $V_8^{(mbe)}$ in equation (39) used in the later surfaces, negative index values are non-physical (as they would lead to interaction energies growing exponentially with distance). For this term, the index range was $(L_{lo}, L_{hi}) = (0, 3)$, with a maximum order $M_{order} = 8$ for the product of the individual distance factors (see § II C 5).

Six fits ("F", "E", "D", "C", "B", and "A"), with four different London cusp-rounding regimes, have similar rms errors (three of these fits are shown in Table II). For each of these, STEPWISE was used to obtain 400-parameter versions of the fits. Several hundred plots of these surfaces were compared, in an attempt to choose between them; the 400-parameter version of surface "A" appeared to yield the best compromise between goodness of fit and lack of spurious wiggles, and was thus chosen as our adopted surface (labelled "Ad").

We have used a large number of linear parameters in order to fit our data. For comparison, Truhlar and Horowitz[37] fitted 287 *ab initio* H_3 points with about 23 parameters to, a

12:1 ratio of points to parameters. Our BKMP2 H_3 surface[22] fitted 8559 H_3 points (7591 *ab initio* points) with about 120 parameters, a 71:1 ratio (63:1 for *ab initio*). Aguado *et al.*[3] fitted 6101 *ab initio* H_4 energies with 865 linear parameters, a 7:1 ratio. The present H_4 surface uses 400 parameters to fit 61547 points (48180 *ab initio* points), giving a ratio of 154:1 (120:1 for *ab initio*). Thus, considering the number of points used to constrain the the fit, 400 parameters does not seem unreasonably high.

C. Checks of the adopted fit

As shown in Table II, the adopted fit has an energy-weighted rms error of 1.15 mE_h with respect to the 48180 *ab initio* energies, comparable to the estimated ~ 1 mE_h error in the *ab initio* energies themselves (see § II B), though larger than the estimated "random" *ab initio* error of ~ 0.5 mE_h. (The unweighted rms error of the fit relative to the *ab initio* energies is 1.43 mE_h.) Figure 2 shows a histogram of the 48180 weighted deviations for the *ab initio* energies [with reduced weights at high energies: see equation (46)] — this is very similar to a histogram of unweighted deviations, since only a small fraction of the *ab initio* energies lie at high enough energies to get reduced weight. At relatively low *ab initio* energies $E \lesssim -0.174$ E_h, below any conical intersection with the first excited state, the rms error is only 0.45 mE_h — again, comparable to the estimated error in *ab initio* energies of points that are tending towards $H_2 + H_2$. At higher energies, the worst points are those on or near the conical intersection with the first excited state, and can have errors as high as ~ 20 mE_h; however, in many cases the surface just "rounds off" the conical intersection somewhat, and in any case the position of the conical intersection comprises only a small portion of the total conformation space. Some spurious wiggles remain in the surface at high energies, but they have been minimized as far as possible.

Figures 3, 4, and 5 show scatterplots of the errors of our adopted surface as a function of *ab initio* energy, for three subsets of the *ab initio* points. The sudden spread in the distributions above about one H_2 dissociation energy (i.e., at $E \gtrsim -0.174$ E_h) is due to the presence of the conical intersection with the first excited state.

1. Examples of the surfaces' worst features

Figure 6 shows an example of the worst of the spurious wiggles present in compact geometries — in this case, for H_2 sizes $r_a = 0.8$ a_0 (very small) and $r_b = 4.0$ a_0 (very large) with small intermolecular separations R. (Two other similar examples are presented in Appendix D in EPAPS[21].) The energy at which the wiggles appear here is $E \sim 0.0$ E_h, i.e., two H_2 dissociation energies above the energy of a pair of separated *equilibrium* H_2 molecules. The energy plotted on the vertical axis is the $H_2 + H_2$ interaction energy for the given H_2-molecule sizes, i.e., the total energy E minus the energy $E_{\rm ref}$ of separated molecules of sizes r_a and r_b. Three different surface fits are shown; each has more structure than required by the *ab initio* data. The adopted 400-parameter surface "Ad" (heavy lines) has wiggles of size $\sim 5 - 10$ mE_h; in this particular case, it is of comparable quality to the 785-parameter surface "A" (medium lines), from which it was obtained ("Ad" does slightly worse for "Y-shape" orientations, but about the same for "T-shape", "parallel", and "crossed"). However,

the surface "G" (light lines), the best of the surfaces that had no London cusp-rounding, does significantly worse than the other two, and also has a small spurious cusp (due to the London component of this surface) at $R \sim 0.25\ a_0$ for the "T-shape" orientation of the H_2 molecules. Note that the plots shown here contain extra-closely-spaced *ab initio* points for illustrative purposes, that were not included in the set of fitted points (they are included among the unfitted "cusp-test" points in Table II — these latter points were used in general to find the position of the conical intersection with the first excited state). The points that were included in the set of fitted points are shown by double-sized symbols in the plots.

Figures 7 – 9 present examples of $H_3 + H$ cases. They show not only the ground state *ab initio* energies but also the first and second excited state energies (though all the second excited state energies lie offscale, except for Fig. 8), revealing conical intersections.

Figure 7 is for T-shaped conformations based on a linearly symmetric H_3. The energy scale on the vertical axis is the interaction energy between a single H atom and a linear symmetric H_3 which has the given interatomic separations $A = B$. It shows an example where the surface "G" is qualitatively correct, but where its London cusp is sufficiently far from the true position of the conical intersection that the surfaces "Ad" and "A" (where this cusp is rounded off) actually do better in fitting the conical intersection. (A similar case where surface "G" does *not* have a cusp is presented in Appendix D in EPAPS[21].)

In Figures 8 and 9, the linear H_3 is replaced with an equilateral triangle (which defines the reference energy). The interaction distance C_{H_3-H} is the distance between the "isolated" H atom and the nearest of the three atoms in the equilateral-triangle H_3.

Figure 8 shows an example of the double conical intersection between the ground state, the first excited state, and the second excited state, where the equilateral-pyramid geometry switches between being singly and doubly degenerate. None of the fitted surfaces do very well for this case; surface "G" fits the double-intersection better than either "Ad" or "A", but contains a spurious 5 mE_h bump in the interaction energy at $C_{H_3-H} \sim 6.5\ a_0$ that is not present in the other two surfaces. The "corner" geometry consists of the same equilateral-triangle base with the fourth atom lying directly above one of the vertices (i.e., a pyramid with the peak displaced); the first excited state for this "corner" geometry lies close in energy to the first excited state of the pyramid geometry, but unlike the pyramid geometry it does *not* experience a crossover between the ground state and the second excited state.

Figure 9 shows an example where the pyramid-conformation conical intersection is fitted reasonably, but a "kite-shaped"-conformation conical intersection is ignored entirely by the fitted surfaces. The "$\Delta\downarrow$" orientation refers to a case where the "isolated" H atom starts at one vertex of the equilateral-triangle H_3 and, as C_{H_3-H} increases, moves away in the plane of the triangle towards and through the mid-point of the opposite side; note that when the H atom is at the center of the triangle ($C_{H_3-H} = 1.501\ a_0$), this orientation corresponds to a pyramid of zero height. This is the conical intersection that is reasonably fitted, although surfaces "Ad" and "A" round it off of course, and surface "G" has a cusp that is too narrow by a factor of ~ 2 in the "$\Delta\downarrow$" orientation. The "kite-shaped"-conformation conical intersection ("$\Delta\downarrow$" orientation at $C_{H_3-H} \sim 3.75\ a_0$) is completely ignored by all fitted surfaces.

Note that the Aguado *et al.*[3] surface also rounds off or ignores the conical intersections, and has some spurious wiggles of comparable magnitude for compact geometries such as those discussed above, though in different regions of conformation space from those where the adopted surface "Ad" has its worst spurious wiggles. However, the Aguado surface is a

rather poorer fit to the *ab initio* energies than the adopted surface. The earlier Keogh[2,4,5] surfaces had much larger spurious wiggles for compact geometries than either the Aguado *et al.*[3] surface or the present adopted surface "Ad".

2. The $H_2 + H_2$ van der Waals well

The $H_2 + H_2$ van der Waals well is fitted quite well by the adopted surface "Ad". For three different relative orientations of a pair of equilibrium H_2 molecules, Figures 10, 11, and 12 compare contour plots of the van der Waals well of the adopted surface "Ad" with the accurate representation from the rigid-rotor $H_2 + H_2$ surface of Schaefer and Köhler[9]. These figures show that surface "Ad" has the bottom of the repulsive wall in the right place and very nearly the correct depth and anisotropy of the van der Waals well, although the outer tail of the van der Waals well is shortened in surface "Ad" due to the fact that it has an exponential cutoff (instead of R^{-6}). As may be seen from Table II (S&K $H_2 + H_2$ with $r_a = r_b = 1.449\ a_0$ and $R \geq 5.9\ a_0$), our adopted surface "Ad" has an rms error in the van der Waals well of 0.007 mE_h, about 5% of the depth of the well itself. This is six times better than the van der Waals rms of the earlier Keogh[2,4,5] surfaces ("Th" and "Tr"), and *very* much better than the behavior of the Aguado *et al.*[3] surface ("ASP"), which is not even qualitatively correct in the van der Waals well region (it has spurious wiggles of order 1 mE_h there). Even the best refitted version ("ASPf") of the Aguado *et al.*[3] surface has an rms error in the van der Waals region of 0.032 mE_h, only slightly better than the earlier Keogh[2,4,5] surfaces ("Th" and "Tr"). These figures also show the $H_2 + H_2$ repulsive wall discussed in III C 4 below. While the Schaefer and Köhler[9] surface is defined down to intermolecular separations of 2 a_0, we show in § III C 4 below that it is not very accurate for interaction energies above 10 mE_h ($R < 4\ a_0$).

3. Other van der Waals regions

Very little information is available about the van der Waals interaction regions of non-equilibrium $H_2 + H_2$, or of $H_3 + H$. As described in § II A 6, we generated energies to constrain non-equilibrium $H_2 + H_2$ by extending the rigid-rotor $H_2 + H_2$ PES of Schaefer and Köhler[9] in a reasonable manner, with reduced weight for non-equilibrium H_2 molecules as described in § II D 1. This ensured that our adopted surface "Ad" was accurate for near-equilibrium $H_2 + H_2$, and at least had qualitatively the correct form even for H_2 sizes fairly far from equilibrium. For extreme cases, namely, $H_2 + H_2$ with both H_2 molecules nearly a factor of 2 either larger or smaller than equilibrium, our fitted surfaces tend to have spurious features of order 0.1 mE_h. However, this is still a very small effect compared to the vibrational or rotational energy of such extreme non-equilibrium H_2 molecules. Likewise, the $H_3 + H$ van der Waals region can only be sampled by high-energy cases where one of the H_2 molecules is in the process of being dissociated. We therefore were satisfied to find that the spurious-appearing features in the $H_3 + H$ van der Waals region of our surfaces tended to have sizes $\lesssim 0.01\ mE_h$ (with features $\sim 0.1\ mE_h$ in only a few cases, mostly when the H_3 was relatively compact). High-energy interactions of hydrogen molecules will sample regions of the surface that have much larger uncertainties than this.

4. The surfaces' best area: the $H_2 + H_2$ repulsive wall

Our adopted surface "Ad" is an extremely good fit to the repulsive wall inside the van der Waals well: as may be seen from Table II (*ab initio* H_4 with "$t < 3.5$", especially the non-compact cases with $A \geq 1.15\ a_0$), the rms error in this region is comparable to the random error in the *ab initio* energies for such conformations. Figure 13 shows this region of surface "Ad" (heavy lines) for several different orientations of a pair of equilibrium H_2 molecules; the Schafer and Köhler rigid-rotor surface[9] is also shown. One can see that the Schafer and Köhler surface behaves rather poorly for interaction energies more than a few tens of mE_h, with errors of 10% to 30% at interaction energies of $\sim 100\ mE_h$ (note that the Schafer and Köhler surface is defined, though not necessarily accurate, down to separations of 2 a_0). The more recent rigid-rotor surface of Diep and Johnson[10] is only defined for $R \geq 2$ Å, i.e., $R \geq 3.78\ a_0$; as one would expect, if one extrapolates this latter surface inwards to $R < 3.78\ a_0$ it can become wildly inaccurate. The Aguado *et al.*[3] surface does fairly well in this region of conformation space, with errors about three times as large as those of the adopted surface "Ad".

5. Fits of subsets of the points

As a check on the reliability of our adopted fit at interstitial geometries, the set of 61547 fitted energies was split into two halves, and each half was fitted separately in the same manner as the fit to the full set (the fits were labelled "A:odd" and "A:even" since the points were sorted according to their positions in the data files). Although fitted to only half of the points, these two surfaces had rms errors with respect to the full data set that were within 1% of the rms of the adopted surface "Ad". For most of the subsets displayed in Table II, surfaces "A:odd" and "A:even" had rms errors that agreed within a few percent or better with those of surface "Ad". The exceptions were the small subsets, where small-number statistics led to variations in the rms of roughly the expected size, namely, "tetrahedra" and "squares" (size $\sim 10/2$ implies variations of $\sim 40\%$) and the equilibrium-H_2 van der Waals well subsets (size $\sim 100/2$ implies variations of $\sim 15\%$). The fact that the half-point fits "A:odd" and "A:even" show no unexpectedly large errors among the unfitted points indicates that we are not over-fitting the data, i.e., the surfaces do not have excessive flexibility for the energies being fitted.

6. Comparison of fits at interstitial geometries

The earlier surfaces of Keogh *et al.*[2,4,5] and of Aguado *et al.*[3] were fitted to the *ab initio* energies of Boothroyd *et al.*[1], which were regularly spaced on a grid in the distance/angle space of H_4 conformations. For these surfaces, one might reasonably worry that large spurious features might exist in regions between grid-points, and in fact some large spurious features were reported by Keogh[2]. For the surfaces of the present work, not only were nearly an order of magnitude more points available to be fitted, but in addition the majority of the *ab initio* points were chosen randomly in conformation space (albeit with a non-uniform distribution). This would be expected to make spurious features much less likely. Nonetheless,

it seemed worthwhile to check this, by comparing different surfaces at interstitial geometries (where no *ab initio* data existed). One million geometries were generated randomly, using an algorithm similar to that used to generate the "random H_4" geometries of § II A 4, but with a longer tail to long distances so as to test van der Waals regions as well. Both for comparisons between different surfaces of the present work and between our surfaces and that of Aguado *et al.*[3], the rms difference between surfaces at the newly-generated interstitial geometries agreed very well (within 10%) with the rms surface differences at a similar subset of the "random H_4" *ab initio* point geometries; there was likewise good agreement for cases tending towards van der Waals regions between rms differences for *ab initio* and non-*ab initio* geometries. The distribution of the differences and the maximum differences were likewise reasonable. This suggests that the interstitial regions of H_4 conformation space are fitted, on average, about as well as the actual *ab initio* points; there is no evidence of spurious features larger than those already found and discussed in § III C 1.

D. Prospects for further improvement

Significant improvements over the adopted surface of this paper are possible, but would require a major effort. Improvements in the van der Waals well and long-range $H_2 + H_2$ interaction region would require the addition of new analytic functions designed for this region; improvements in the van der Waals well for non-equilibrium H_2-molecule sizes would also require highly accurate *ab initio* computations for a significant number of conformations in the relevant regions. Significant improvements in the interaction region would require not only a greatly improved functional form (e.g., one that takes into account the position and form of the conical intersection with the first excited state), but also an increase by at least an order of magnitude in the number of *ab initio* energies (with accuracy comparable to those of this paper), to improve the coverage in the 6-dimensional conformation space of H_4 and to map out more fully the conical intersection.

IV. CONCLUSIONS

The original 6101 *ab initio* energies reported by Boothroyd *et al.*[1] were checked for correctness, and 9 erroneous energy values were found and corrected. These were supplemented by 42079 newly calculated *ab initio* energies, plus an additional 13367 conformations generated to constrain the fit in regions where the energy could not be obtained directly from our *ab initio* computations. A new analytical H_4 potential energy surface (the surface "Ad" described above) was fitted to these energies. It has an rms error comparable to the error in the *ab initio* energies, namely an energy-weighted rms of 1.15 mE_h for all 48180 *ab initio* energies (unweighted rms of 1.43 mE_h), and of 0.45 mE_h for the 14513 *ab initio* energies below the H_2 dissociation energy. This new H_4 surface is a significant improvement on the surfaces that had been fitted to the original 6101 *ab initio* energies of Boothroyd *et al.*[1], namely, the many-body expansion surface of Aguado *et al.*[3], the H_4 surface of Keogh[2], and a slightly improved version of this latter used for semi-classical trajectory calculations by Martin *et al.*[4] and Mandy *et al.*[5].

For relatively compact conformations, i.e., for energies higher than the H_2 dissociation energy, the conical intersection between the ground state and the first excited state is the largest source of error in the analytic surfaces. The fact that the analytical surfaces "round off" the conical intersection for many geometries results in an error $\gtrsim 2\ mE_h$ over of order 0.1% of that volume of conformation space that has significant interaction energy, with maximum errors up to $\sim 20\ mE_h$. This conical intersection forms a somewhat complicated 3-dimensional hypersurface in the 6-dimensional conformation space of H_4. The present paper has mapped out a large portion of the locus of this conical intersection (see Appendix C in EPAPS[21]). However, trying to include the conical intersection explicitly in the analytic H_4 surface would require a major effort, both to map its position and shape in more detail, and to fit its geometry to some analytic form.

Our adopted surface "Ad" fits the van der Waals well to an rms accuracy of about 5% and behaves reasonably for non-equilibrium H_2-molecule sizes (although it has an exponential cutoff at large intermolecular separation R, rather than dying away as R^{-6}). For equilibrium-size H_2 molecules at large separations ($R \gtrsim 4\ a_0$, or interaction energies $\lesssim 10\ mE_h$), the rigid-rotor $H_2 + H_2$ surfaces of Schaefer and Köhler[9] or of Diep and Johnson[10] are somewhat more accurate than the adopted H_4 surface of the present work. However, the rigid-rotor surfaces are defined only for equilibrium H_2 molecules; in addition, they can be significantly in error (by $\gtrsim 10\%$) in the $H_2 + H_2$ repulsive wall at $R \lesssim 3.5\ a_0$ or at interaction energies $\gtrsim 30\ mE_h$, regions where our adopted surface is very accurate.

A Fortran program version of the adopted surface "Ad" of the present work, including analytical first derivatives, is available from EPAPS[21]. Files containing the *ab initio* energies (either ground state energies only, or all computed MRD-CI roots) are also available from EPAPS[21] (as are the H_3 Fortran programs and *ab initio* energies, and Appendices A through D). These Fortran programs and files of *ab initio* energies can also be obtained from the authors[38].

ACKNOWLEDGMENTS

This work was supported by the Natural Sciences and Engineering Research Council of Canada.

REFERENCES

[1] A. I. Boothroyd, W. J. Keogh, P. G. Martin, and M. J. Peterson, J. Chem. Phys. **95**, 4331 (1991).

[2] W. J. Keogh, Ph. D. Thesis, University of Toronto (1992).

[3] A. Aguado, C. Suarez, and M. Paniagua, J. Chem. Phys. **101**, 4004 (1994).

[4] P. G. Martin, W. J. Keogh, and M. E. Mandy, Astrophys. J. **499**, 793 (1998).

[5] M. E. Mandy, P. G. Martin, and W. J. Keogh, J. Chem. Phys. **108**, 492 (1998).

[6] J. E. Dove, A. C. M. Rusk, P. H. Cribb, and P. G. Martin, Astrophys. J. **318**, 379 (1987).

[7] C. A. Chang and P. G. Martin, Astrophys. J. **378**, 202 (1991).

[8] P. G. Martin, D. H. Schwarz, and M. E. Mandy, Astrophys. J. **461**, 265 (1996).

[9] J. Schaefer and W. E. Köhler, Z. Phys. **D 13**, 217 (1989).

[10] P. Diep and J. K. Johnson, J. Chem. Phys. **112**, 4465 (2000).

[11] G. D. Billing and R. E. Kolesnick, Chem. Phys. Lett. **215**, 571 (1993).

[12] G. D. Billing, Chem. Phys. **20**, 35 (1977).

[13] D. W. Schwenke, J. Chem. Phys. **89**, 2076 (1988).

[14] D. W. Schwenke, private communication (1989).

[15] P. G. Burton and U. E. Senff, J. Chem. Phys. **76**, 6073 (1982).

[16] P. G. Burton and U. E. Senff, J. Chem. Phys. **79**, 526 (1983).

[17] U. E. Senff and P. G. Burton, Aust. J. Phys. **42**, 47 (1989).

[18] U. Buck, F. Huisken, J. Schleusener, and J. Schaefer, J. Chem. Phys. **74**, 535 (1981).

[19] U. Buck, F. Huisken, G. Maneke, and J. Schaefer, J. Chem. Phys. **74**, 4430 (1981).

[20] U. Buck, F. Huisken, A. Kolhase, D. Otten, and J. Schaefer, J. Chem. Phys. **78**, 4439 (1983).

[21] See EPAPS Document No. E-JCPSA6-115-304140 for Appendices A through D to this paper, as well as for Fortran programs to compute the adopted H_4 and H_3 surfaces (including first derivatives), and files of *ab initio* H_4 and H_3 energies. This document may be retrieved via the EPAPS homepage (`http://www.aip.org/pubservs/epaps.html`) or from `ftp.aip.org` in the directory `/epaps/`. See the EPAPS homepage for more information.

[22] A. I. Boothroyd, W. J. Keogh, P. G. Martin, and M. R. Peterson, J. Chem. Phys. **104**, 7139 (1996).

[23] H. Partridge, C. W. Bauschlicher, J. R. Stallcop, and E. Levin, J. Chem. Phys. **99**, 5951 (1993).

[24] H. Partridge, private communication: H_2 energies (1992) and H_3 energies (1994).

[25] A. I. Boothroyd, W. J. Keogh, P. G. Martin, and M. R. Peterson, J. Chem. Phys. **95**, 4343 (1991).

[26] R. J. Buenker, private communication (1987).

[27] R. J. Buenker and P. Funke, private communication (1992).

[28] P. Siegbahn and B. Liu, J. Chem. Phys. **68**, 2457 (1978).

[29] M. Paniagua and A. Aguado, private communication (1994).

[30] P. G. Burton, S. D. Peyerimhoff, and R. J. Buenker, Chem. Phys. **73**, 83 (1982).

[31] P. G. Burton, Int. J. Quantum Chem. **23**, 613 (1983).

[32] P. G. Burton, R. J. Buenker, P. J. Bruna, and S. D. Peyerimhoff, Chem. Phys. Lett. **95**, 379 (1983).

[33] I. Shavitt, F. B. Brown, and P. G. Burton, Int. J. Quantum Chem. **31**, 507 (1987).
[34] N. J. Brown and D. M. Silver, J. Chem. Phys. **65**, 311 (1976).
[35] B. R. Johnson, J. Chem. Phys. **74**, 754 (1981).
[36] R. Rydberg, Z. Phys. **73**, 25 (1931).
[37] D. G. Truhlar and C. J. Horowitz, J. Chem. Phys. **68**, 2466 (1978); J. Chem. Phys. **79**, 1514 (1979: Errata).
[38] A Fortran program of the adopted surface, or files of *ab initio* energies, can also be obtained by contacting P. G. Martin, email: `pgmartin@cita.utoronto.ca` and/or visiting the website `http://www.cita.utoronto.ca/~pgmartin/h4pes`.

TABLES

TABLE I. Values of non-linear parameters used in the best of the fitted H_4 surfaces.

Surface	Parameter Values				
ASPo	$\beta_p = 1.404\ a_0^{-1}$				
ASPa	$\beta_p = 1.404\ a_0^{-1}$				
ASPf	$\beta_p = 1.28\ a_0^{-1}$				
All[a]	$A_{p_2} = 0.2593\ a_0^{-A_{p3}}$	$S_1^o = 10.04$	$S_1^t = 0.312\ a_0^{-1}$	$S_1^u = 1.61\ a_0^{-1}$	
	$A_{p_3} = 1.6813$	$S_2^o = 4.03$	$S_2^t = 0.53\ a_0^{-1}$	$S_2^u = 1.079\ a_0^{-1}$	
Best[b]	$\beta_1 = 0.006\ a_0^{-3}$	$\beta_2 = 0.006\ a_0^{-3}$	$\beta_3 = 0.006\ a_0^{-3}$	$\beta_4 = 0.006\ a_0^{-3}$	
	$\beta_5 = 0.006\ a_0^{-3}$	$\beta_6 = 0.003\ a_0^{-3}$	$\beta_7 = 0.006\ a_0^{-3}$	$C_{\epsilon\Delta} = 3.0\ a_0$	$\beta_J = 10.0$
G[c]	$C_{\epsilon E} = 0.0\ E_h$	$C_{\epsilon S} = 0.0\ a_0$	$C_{\epsilon W} = 0.0\ a_0$	$\beta_8 = 0.006\ a_0^{-3}$	
F	$C_{\epsilon E} = 0.073\ E_h$	$C_{\epsilon S} = 6.0\ a_0$	$C_{\epsilon W} = 1.5\ a_0$	$\beta_8 = 0.006\ a_0^{-3}$	
E	$C_{\epsilon E} = 0.181\ E_h$	$C_{\epsilon S} = 5.5\ a_0$	$C_{\epsilon W} = 1.5\ a_0$	$\beta_8 = 0.006\ a_0^{-3}$	
D	$C_{\epsilon E} = 0.368\ E_h$	$C_{\epsilon S} = 4.0\ a_0$	$C_{\epsilon W} = 4.0\ a_0$	$\beta_8 = 0.006\ a_0^{-3}$	
C	$C_{\epsilon E} = 0.775\ E_h$	$C_{\epsilon S} = 3.75\ a_0$	$C_{\epsilon W} = 3.75\ a_0$	$\beta_8 = 0.006\ a_0^{-3}$	
B[d]	$C_{\epsilon E} = 0.075\ E_h$	$C_{\epsilon S} = 6.0\ a_0$	$C_{\epsilon W} = 1.5\ a_0$	$\beta_8 = 0.0\ a_0^{-3}$	$\beta_p = 0.8\ a_0^{-1}$
A[d]	$C_{\epsilon E} = 0.775\ E_h$	$C_{\epsilon S} = 3.75\ a_0$	$C_{\epsilon W} = 3.75\ a_0$	$\beta_8 = 0.0\ a_0^{-3}$	$\beta_p = 0.8\ a_0^{-1}$

[a]Except for the refits of the Aguado *et al.*[3] surface, all of our surface fits used these parameters.
[b]Although a number of earlier fits had of course been made to test other sets of β values, all of the "best" fits (with good rms values and not too many spurious wiggles) used this set of β values; note that the β_6 value (for term selecting "non-linear $H_3 + H$") differs from the others.
[c]Surface "G" is the best of the surfaces that have no London cusp-rounding, i.e., for which these cusp-rounding parameters are zero.
[d]In surfaces "B" and "A" the "compact" term V_8 is replaced with the relatively low-order many-body expansion term $V_8^{(mbe)}$. Note that the adopted surface "Ad" is the the 400-parameter version of surface "A".

TABLE II. Energy-weighted[a] rms errors of fitted surfaces, in mE_h.

Surface I.D.:[b]		Th	Tr	ASP	ASPo	ASPa	ASPf	G	F	C	A	Cd	Ad
No. of linear parameters:		400	400	865	365+	370+	351	791	790	792	785	400	400
Subset	N_{pts}	rms	rms	rms	rms	rms	rms	rms	rms	rms	rms	rms	rms
All *ab initio* H_4	48180	3.52	2.82	4.13	4.05	*2.61*	3.12	1.39	1.13	1.12	1.07	1.19	1.15
... $E < 0.0\ E_h$[c]	39061	2.06	2.01	2.92	2.87	2.31	2.64	1.16	0.96	0.96	0.89	1.00	0.95
... $E < -0.174\ E_h$[d]	14513	1.05	1.08	1.56	1.44	1.33	1.64	0.50	0.48	0.48	0.41	0.49	0.45
... $A < 0.95\ a_0$	11712	5.34	3.64	6.69	6.59	2.99	3.94	1.66	1.29	1.28	1.25	1.39	1.35
... $A \geq 0.95\ a_0$	36468	2.69	2.50	2.85	2.78	2.48	2.80	1.29	1.07	1.07	1.01	1.13	1.08
... $A < 1.15\ a_0$	18198	5.03	3.73	5.67	5.58	2.83	3.66	1.67	1.30	1.29	1.28	1.39	1.37
... $A \geq 1.15\ a_0$	29982	2.13	2.08	2.80	2.73	2.47	2.73	1.19	1.01	1.01	0.93	1.05	0.99
... $t \geq 3.5$[e]	40249	3.82	3.06	4.34	4.25	2.78	3.29	1.50	1.21	1.21	1.16	1.29	1.24
... $t < 3.5$[e]	7931	1.08	0.95	2.84	2.86	1.47	2.03	0.52	0.49	0.49	0.44	0.50	0.46
... ... $A < 1.15\ a_0$	4225	1.34	1.14	3.77	3.83	1.85	2.66	0.60	0.57	0.56	0.52	0.58	0.54
... ... $A \geq 1.15\ a_0$	3706	0.67	0.65	0.99	0.90	0.86	0.87	0.40	0.39	0.39	0.33	0.40	0.36
... "random" H_4	27585	2.53	2.24	3.36	3.29	2.31	2.46	1.13	0.94	0.94	0.85	0.98	0.91
... Original H_4	6101	1.94	2.17	1.95	*1.79*	2.75	4.39	1.64	1.38	1.38	1.36	1.48	1.48
... Schwenke's H_4	87	2.21	2.23	1.99	1.97	2.14	2.25	0.74	0.71	0.73	0.56	0.65	0.52
... Tetrahedra	10	4.34	4.11	6.67	6.97	10.46	20.14	2.07	2.60	2.49	2.12	2.26	1.89
... Squares	11	3.26	3.72	2.49	2.59	6.27	10.51	1.24	1.21	1.27	1.10	1.95	2.36
... $H_4 \rightarrow H_3 + H$	2500	5.95	5.57	3.80	3.78	3.30	2.83	2.11	1.38	1.31	1.26	1.36	1.29
... ... $A < 1.15\ a_0$	1613	6.91	6.46	4.05	4.02	3.35	2.66	2.47	1.55	1.47	1.39	1.52	1.43
... ... $A \geq 1.15\ a_0$	887	3.57	3.39	3.30	3.29	3.21	3.12	1.20	0.98	0.96	0.97	1.00	0.99
S&K H_2+H_2	3611	.779	.775	1.256	1.255	.630	.280	.188	.173	.172	.137	.162	.152
... $r_a, r_b = 1.449\ a_0$	224	.077	.082	.422	.378	.356	.120	.078	.071	.072	.037	.075	.047
... ... $R < 5.9\ a_0$	79	.115	.124	.399	.311	.309	.197	.122	.110	.113	.062	.117	.078
... ... $R \geq 5.9\ a_0$	145	.044	.044	.434	.410	.378	.032	.035	.035	.035	.006	.035	.007
H_4fromH_3	8559	.829	.829	1.395	1.395	1.395	1.395	.200	.200	.200	.200	.200	.200
"Cusp-test" H_4[f]	13356	8.95	8.87	11.06	11.49	11.60	14.67	8.14	7.69	7.64	7.66	7.91	8.03
... $E < 0.0\ E_h$[c,f]	11887	8.82	8.78	10.90	11.32	11.73	14.95	8.12	7.67	7.64	7.63	7.92	8.03
Fitted full-weight[a]	61547	5.45	5.12	12.28	11.88	9.60	*6.11*	*1.70*	*1.53*	*1.53*	*1.33*	*1.58*	*1.38*

[a]For energy-weighted rms errors, deviations only get weight w_E from equation (46), as opposed to full-weight rms errors in last line of table; *italics:* rms values minimized by the fitting procedure.
[b]Surfaces of Keogh[2] ("Th"), modified Keogh[4,5] ("Tr"), Aguado *et al.*[3] ("ASP"), and present work: differential refits of Aguado *et al.*[3] surface to old H_4 points ("ASPo") and to all *ab initio* points ("ASPa"), and refit to *full* dataset ("ASPf"); our best without London cusp-rounding ("G"), 3 of 6 "best" fits ("F", "C", and "A"), and 2 reduced-parameter fits ("Cd" and adopted fit "Ad").
[c]H_4 energy less than twice the H_2 dissociation energy, relative to a pair of equilibrium H_2 molecules.
[d]H_4 energy less than the H_2 dissociation energy.
[e]The selector t is defined as $t = (r_a + r_b) \sum_{i \neq a,b} (1/r_i)$, so small values of t select conformations tending towards separated $H_2 + H_2$: for $r_a \sim r_b$, requiring $t < 3.5$ selects $R \gtrsim r_a + r_b$.
[f]These "cusp-test" points were *not* fitted; most lie on or near the conical intersection with the first excited state (a sharp cusp that is not in the surfaces' functional form, yielding a poor fit there).

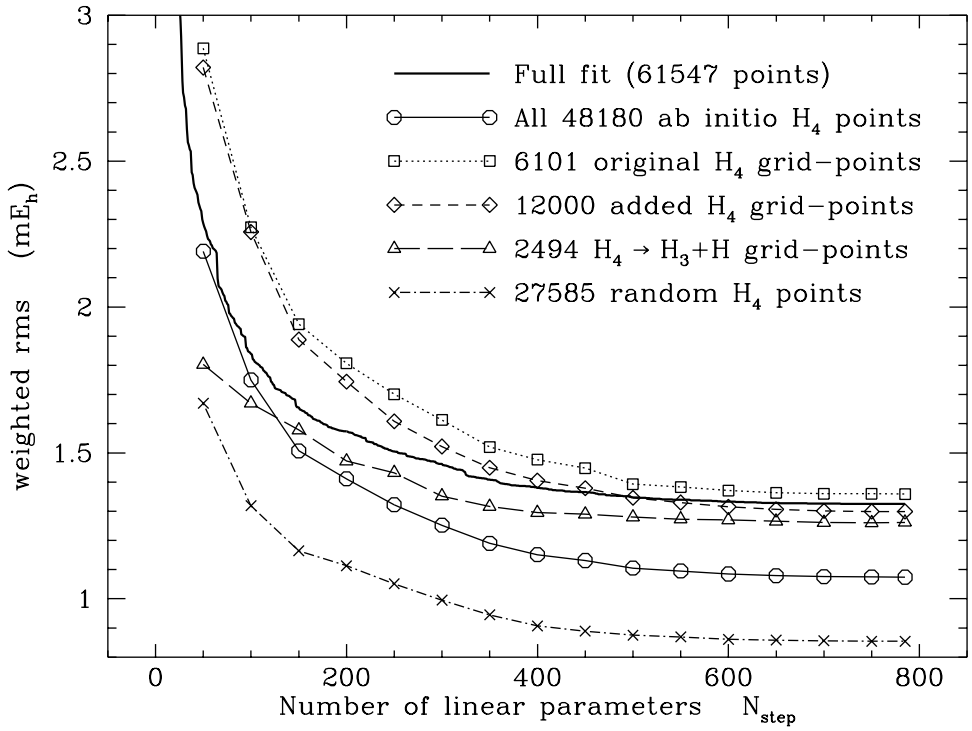

FIG. 1. Rms error as a function of the number of linear parameters N_{step} kept by STEPWISE, for the fit "A"; the adopted surface "Ad" corresponds to $N_{step} = 400$. Heavy solid line indicates the weighted rms error of the full fit. Other lines, with symbols, indicate the rms error of various subsets of *ab initio* points, at every 50^{th} step; these latter are "energy-weighted" rms values, the weight being unity except at high energies (see § II D 1).

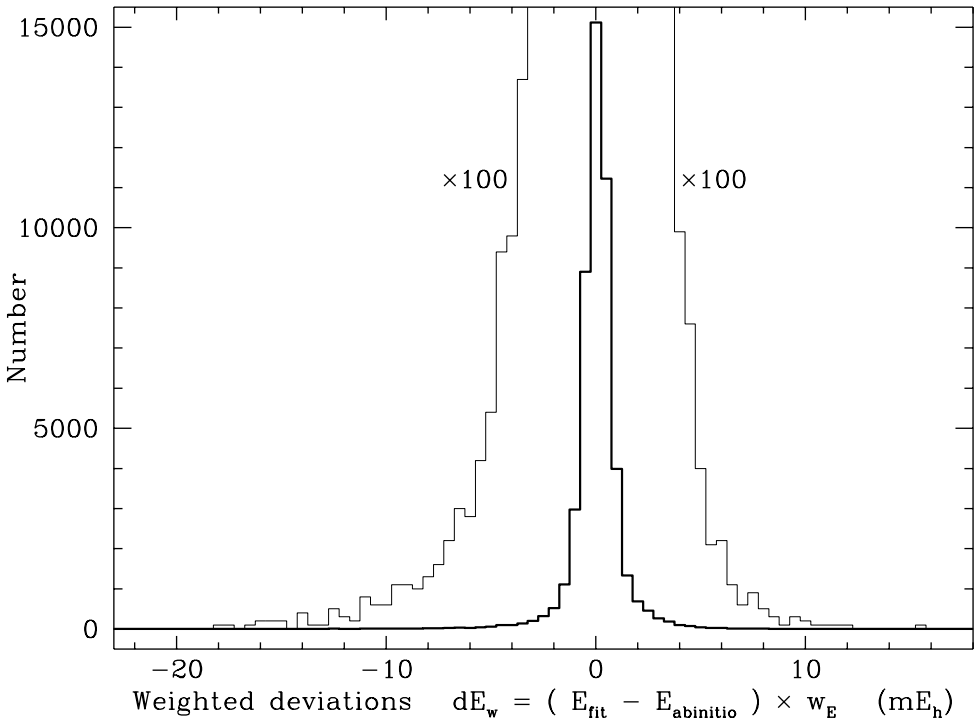

FIG. 2. Histogram of the energy-weighted deviations of our adopted surface "Ad", for the 48180 *ab initio* energies [see equation (46)].

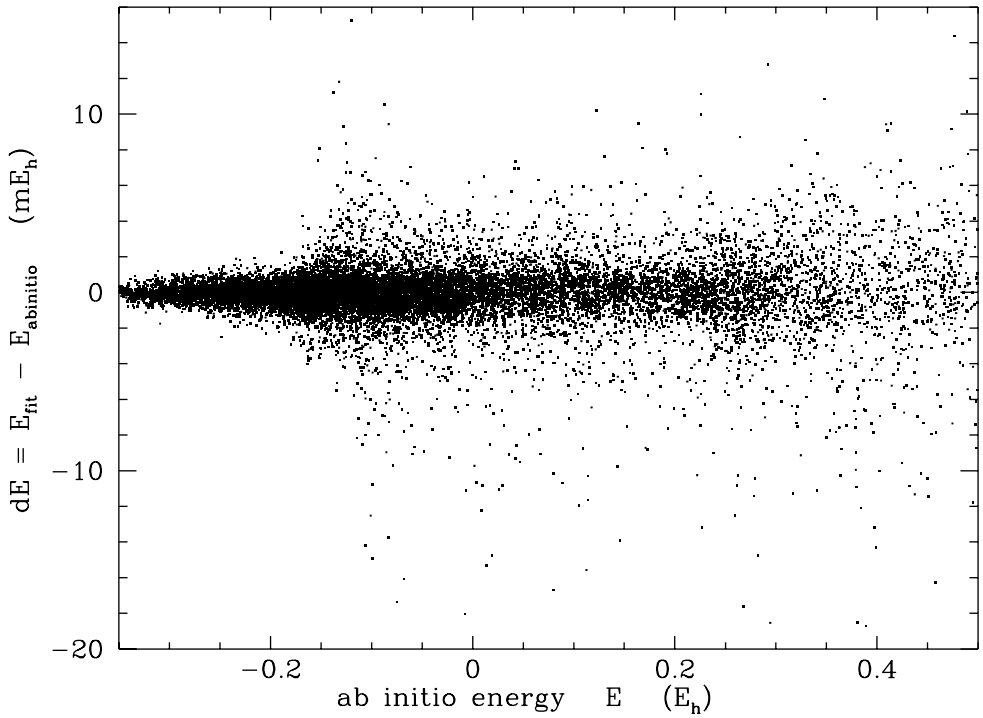

FIG. 3. Scatterplot of the unweighted errors of our adopted surface "Ad", as a function of the *ab initio* energy, for the 6101 points in the original grid plus the 12000 added points described in § II A 1 and II A 3 (not including the 2494 added $H_4 \rightarrow H_3 + H$ points of § II A 2 or the large random set of § II A 4). Energies are measured relative to that of four isolated hydrogen atoms. Note that a few hundred high-energy points with $E > 0.5\ E_h$ lie offscale to the right — their distribution in dE remains within the same bounds as that for $E < 0.5\ E_h$, but is of course less densely populated.

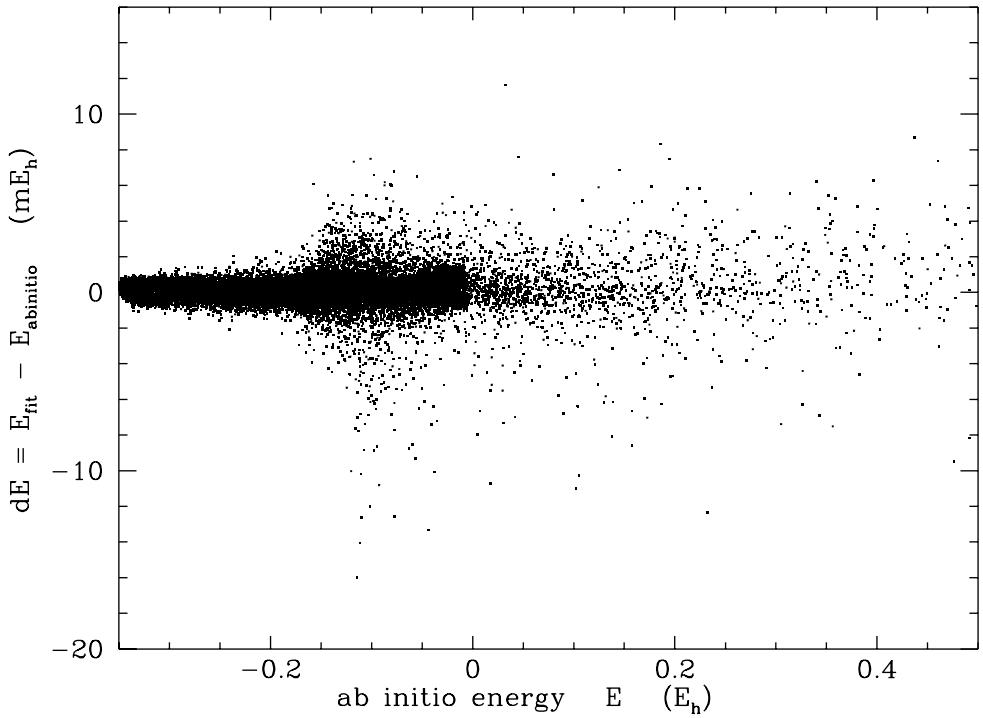

FIG. 4. Scatterplot of the unweighted errors of our adopted surface "Ad", as a function of the *ab initio* energy, for the 27585 "random" H_4 points of § II A 4. The distribution in conformation space is such that the majority of these points have energies $E \lesssim 0.0\ E_h$. Note that several dozen high-energy points with $E > 0.5\ E_h$ lie offscale to the right.

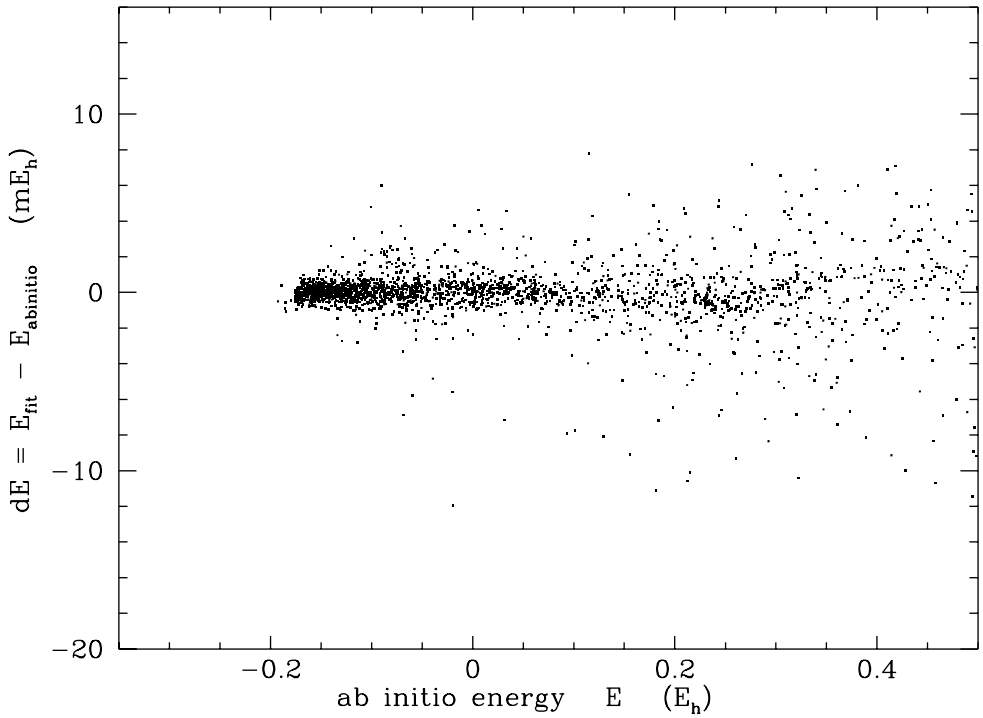

FIG. 5. Scatterplot of the unweighted errors of our adopted surface "Ad", as a function of the *ab initio* energy, for the 2494 $H_4 \rightarrow H_3 + H$ points of § II A 2. Note that a few dozen high-energy points with $E > 0.5\ E_h$ lie offscale to the right.

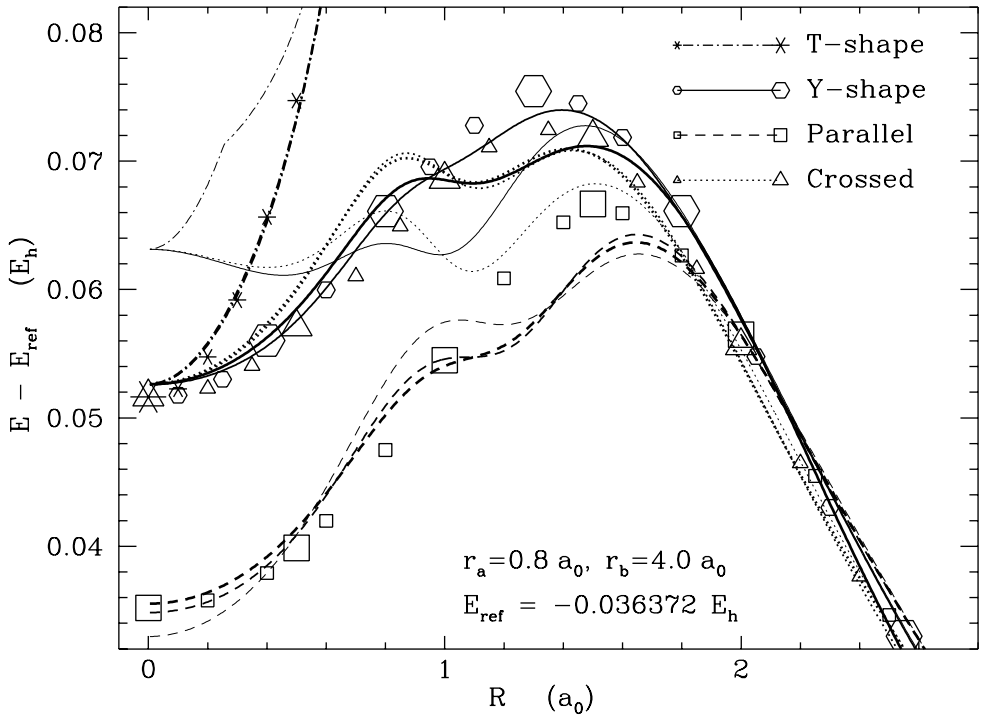

FIG. 6. An example of spurious wiggles in the fitted surface, for fairly compact geometries, as a function of the distance R between the centers of a short and a long H_2 "molecule" (sizes $r_a = 0.8\ a_0$ and $r_b = 4.0\ a_0$; this conformation has energy $E_{\rm ref}$ for $R \to \infty$). Discrete symbols indicate *ab initio* energies (double-sized symbols indicate fitted points; others are extra "test" points). Heavy curves show surface "Ad" (the adopted surface, with 400 parameters), medium curves show the corresponding 785-parameter surface "A", and light curves show the 791-parameter surface "G" (the best of the surfaces that had no London cusp-rounding). The "parallel" case refers to the case with $\vec{r}_a \parallel \vec{r}_b \perp \vec{R}$. The other three are cases with $\vec{r}_a \perp \vec{r}_b$, forming a "+" shape at $R = 0$; the "Y-shape" has $\vec{r}_a \parallel \vec{R}$, the "T-shape" has $\vec{r}_b \parallel \vec{R}$, and the "crossed" case has $\vec{r}_a \perp \vec{R} \perp \vec{r}_b$.

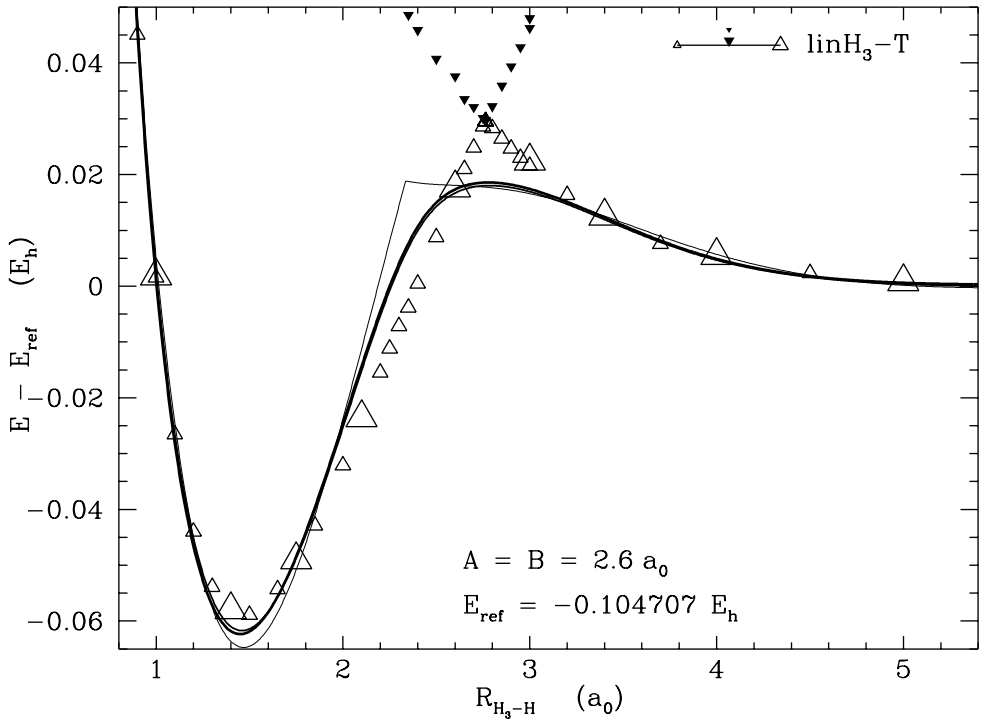

FIG. 7. An example where London cusp-rounding (in the adopted surface "Ad" and in surface "A") smoothes out a cusp (in surface "G") that is somewhat out of position, yielding some improvement. For this "LinH$_3$-T" orientation, the distance R_{H_3-H} is that between a fourth H atom and the central atom of a linear-symmetric H_3 (that has interatomic separations $A = B = 2.6\ a_0$), with $\vec{A} \parallel \vec{B} \perp \vec{R}_{\mathrm{H_3-H}}$, forming a T-shape with respect to the linear H_3 (this conformation has energy E_{ref} for $R_{\mathrm{H_3-H}} \to \infty$). Symbols for *ab initio* energies of the first and second excited states (in this case, larger and smaller solid triangles, respectively) are indicated immediately above the middle of the line-type legend (note that all second excited state energies lie offscale in this figure). Heavy, medium, and light curves show surfaces "Ad", "A", and "G", respectively, as in Fig. 6.

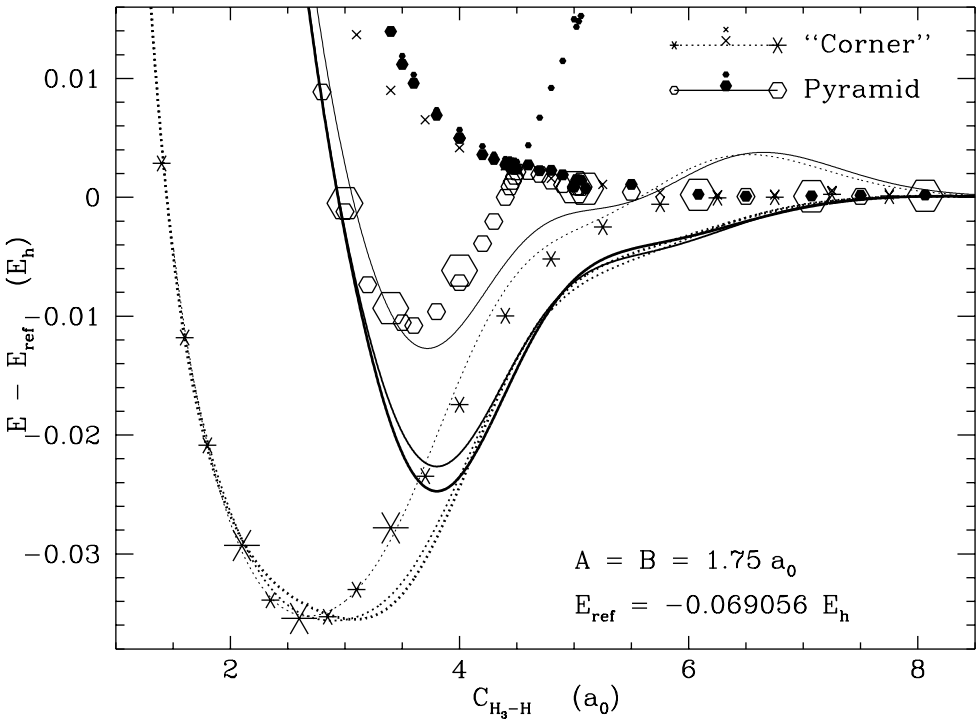

FIG. 8. An example of the double conical intersection between the ground state, the first excited state, and the second excited state (where the equilateral-pyramid geometry switches between being singly and doubly degenerate). The first three atoms form an equilateral triangle with sides of 1.75 a_0; $C_{\mathrm{H_3-H}}$ is the distance from the fourth atom to a vertex of the equilateral triangle (this conformation has energy E_{ref} for $C_{\mathrm{H_3-H}} \to \infty$). For the "corner" case, the fourth atom lies directly above one vertex of the triangle; for the "pyramid" case, the fourth atom lies directly above the center of the triangle. Heavy, medium, and light curves show surfaces "Ad", "A", and "G", respectively, as in previous figures.

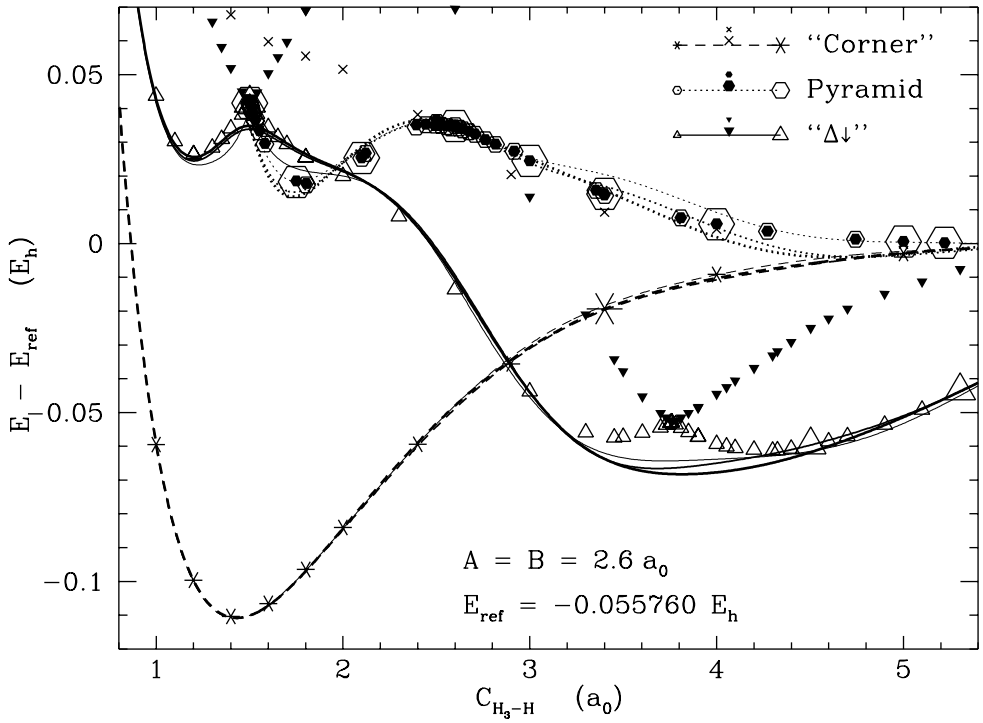

FIG. 9. An example where the pyramid conical intersection is fit relatively well, but another "kite-shaped" conical intersection ("$\Delta\downarrow$" at $C_{H_3-H} \sim 3.8\ a_0$) is completely ignored by the fitted surfaces. Notation as in Fig. 8, except that the size of the equilateral triangle H_3 is 2.6 a_0; also, the added curve labelled "$\Delta\downarrow$" refers to a case where the fourth atom starts at one vertex of the triangle (for $C_{H_3-H} = 0$) and moves away in the plane of the triangle towards and through the mid-point of the opposite side as C_{H_3-H} increases. Heavy, medium, and light curves show surfaces "Ad", "A", and "G", respectively, as in previous figures.

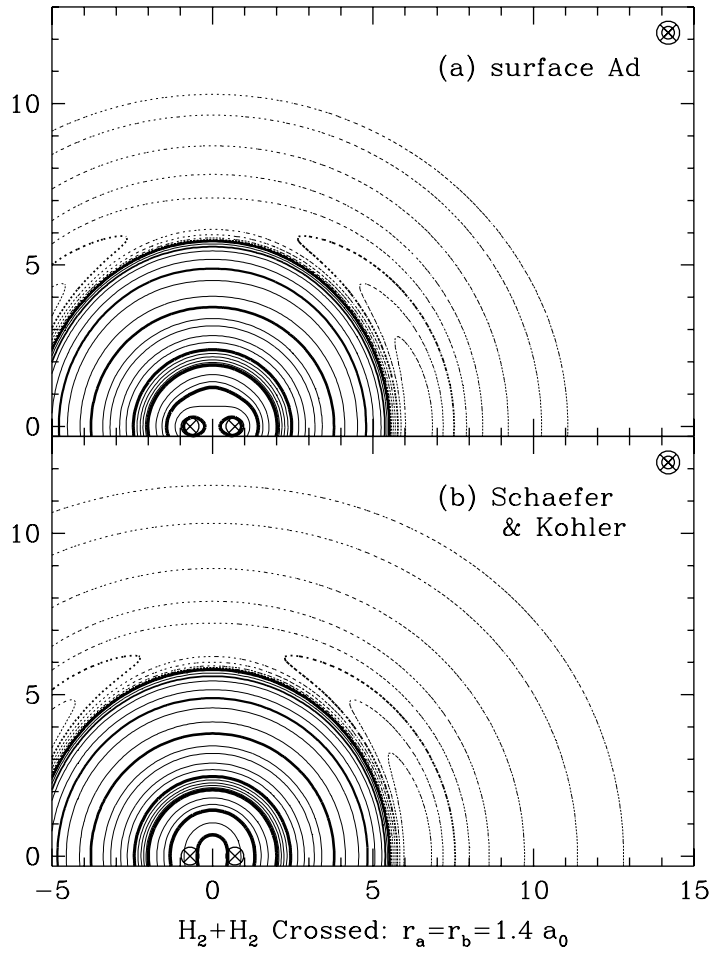

FIG. 10. Contour plot of the van der Waals well and repulsive wall of $H_2 + H_2$ with equilibrium H_2 molecules, as a function of the intermolecular separation R (in a_0), for the "crossed" orientation of the H_2 molecules: $\vec{r}_b$ is perpendicular to the plane defined by $\vec{r}_a$ and the intermolecular separation $\vec{R}$. Comparison of (a) the adopted surface "Ad", and (b) the Schaefer and Köhler rigid-rotor surface[9]. Dashed lines indicate negative interaction energies, at contour levels $\{-0.005,\ -0.010,\ -0.025,\ -0.050,\ -0.075,\ \textit{−0.100},\ -0.125,\ -0.150,\ -0.175\}$ mE_h; solid lines indicate positive interaction energies, at contour levels $\{$ *0.0*, 0.005, 0.01, 0.02, 0.05, *0.1*, 0.2, 0.5, *1*, 2, 5, *10*, 20, 30, 50, 70, *100*, 120, 140, 160, 180, *200*, 300, 400, *500*, 750, *1000* $\}$ mE_h (*italics* correspond to heavy contour lines). Positions of the atoms in the first H_2 molecule $\vec{r}_a$ are indicated by the symbols $\otimes$ near the origin. Orientation of the second H_2 molecule $\vec{r}_b$ is indicated by the symbols $\otimes$ at upper right (different sizes of the symbols $\otimes$ indicate displacement into and out of the plane of the page). While the Schaefer and Köhler surface is defined down to intermolecular separations of 2 a_0, it is not very accurate for interaction energies above 10 mE_h ($R < 4\ a_0$ — see III C 4), so its inner contour lines are not relevant.

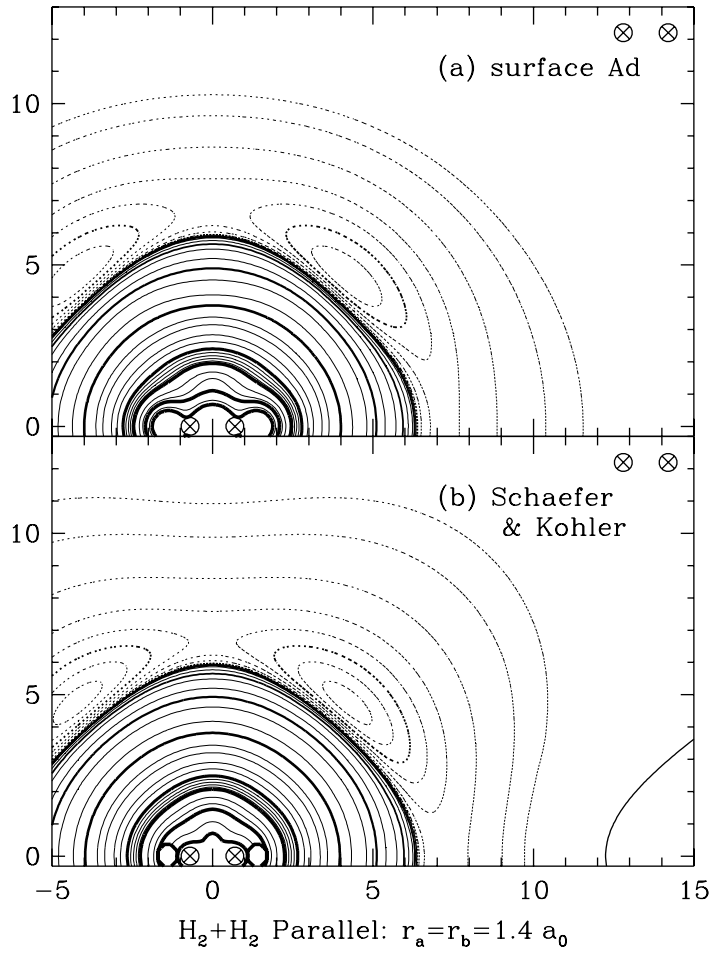

FIG. 11. Contour plot of the van der Waals well and repulsive wall of $H_2 + H_2$ (similar to Fig. 10), for the "parallel" orientation of the H_2 molecules: $\vec{r}_a \parallel \vec{r}_b$ (with $\vec{R}$ in the same plane). The solid contour to the lower right (and upper right in the following figure) is curious but the Diep and Johnson[10] rigid-rotor surface also has regions of positive interaction energy in about the same places (though with slightly less regular edges).

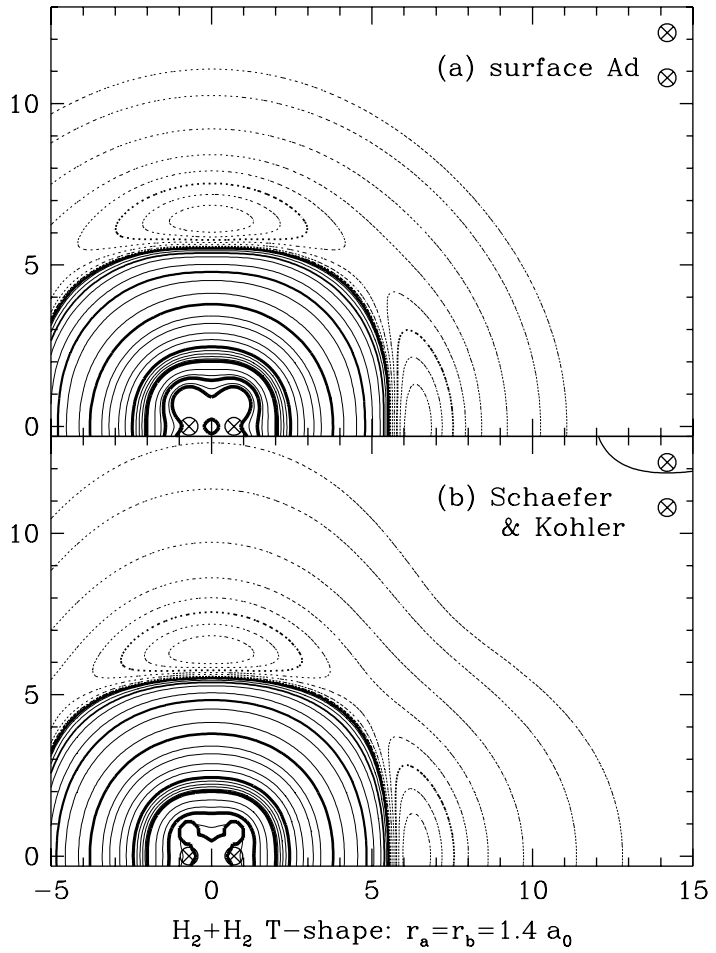

FIG. 12. Contour plot of the van der Waals well and repulsive wall of $H_2 + H_2$ (similar to Fig. 10), for the "T-shape" orientation of the H_2 molecules: $\vec{r}_a \perp \vec{r}_b$ (with $\vec{R}$ in the same plane).

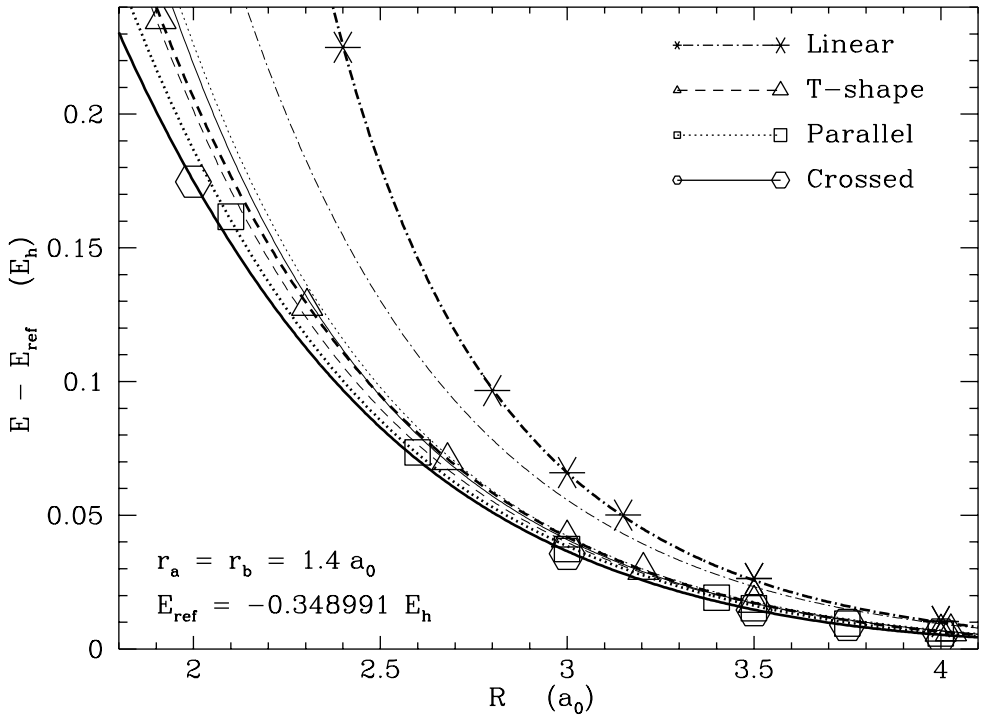

FIG. 13. The repulsive wall of $H_2 + H_2$, showing *ab initio* energies (discrete symbols), the adopted surface "Ad" (heavy lines), and the Schaefer and Köhler rigid-rotor surface[9] (light lines) — notation as in Fig. 6.